Aseismic Design of Underground Structures

C. M. St John and T. F. Zahrah

Abstract—*This study defines the basis for the aseismic design of subsurface excavations and underground structures. It includes a definition of the seismic environment and earthquake hazard, and a review of the analytical and empirical tools that are available to the designer concerned with the performance of underground structures subjected to seismic loads. Particular attention is devoted to development of simplified models that appear to be applicable in many practical cases.*

Résumé—*Cette étude définit les bases pour la conception aséismique d'excavations et de structures sous-terre. On inclut une définition de l'environnement séismique et du risque de tremblement de terre, ainsi qu'une revue des techniques analytiques et empiriques qui sont à la disposition du concepteur préoccupé de la performance des structures sous terre et soumises à des actions séismiques. Une attention particulière est donnée au développement de modèles simplifiés qui semblent être applicables dans la plupart du temps.*

Introduction

The objective of this report is to provide a relatively concise statement of the state of the art for the design of underground structures in seismic environments. Like many other state-of-the-art reports, it is intended to be brief and to focus on recommended practice. Its intended audience is the practicing engineer who may have extensive experience in the design of underground structures but who has limited awareness of the special considerations necessary in a seismically active environment.

The need to establish a consensus on seismic design procedures for underground structures has been recognized for a number of years. In 1980, the International Tunnelling Association established a working group on the topic. Since that time, the group has met regularly to discuss progress in collection of case histories and preparation of appropriate documentation and design recommendations. During this study we have drawn heavily on the activities of that working group, and have benefited significantly from the level of international cooperation it has engendered. To what extent this report satisfies the need for a seismic design manual, and reflects the opinions of the international tunnelling community, remains to be determined.

The remainder of the report comprises four sections, four appendices, and a bibliography. The extensive use of Appendices reflects a desire to keep the main text brief, without leaving the reader with an incomplete treatment. Specifically, the next section, on subject of seismic environment, is amplified in Appendix A; and the last section, in which simplified design procedures are recommended, is supported by Appendices B and C, which cover theoretical developments, and Appendix D, which contains design examples. The third section summarizes the current empirical base for design of underground structures in rock, and the fourth section briefly reviews the analytical tools available to the tunnel engineer concerned with design in a seismic environment. Needless to say, this report cannot be entirely comprehensive. However, we believe it provides a basis for understanding the issues involved in seismic design, as well as a rational approach that may prove satisfactory in many cases of practical concern.

This report was prepared by the authors for the ITA Working Group on Seismic Effects on Underground Structures, under National Science Foundation Grant No. CEE-8310631. The report was published originally by Agbabian Associates, El Segundo, California (U.S.A.). We are grateful to the National Science Foundation for granting permission to publish the report in this publication.

Seismic Activity

This chapter contains a brief summary of the fundamental concepts pertaining to the definition of the seismic environment and the development of seismic input criteria for the design of underground structures. The subject is more fully addressed in Appendix A.

Seismic Environment

Seismologists typically classify earthquakes according to four modes of generation—tectonic, volcanic, collapse, or explosion. Regardless of the type of earthquake, an engineer concerned with design of underground structures requires that the seismic environment be defined in a quantitative manner. Specifically, the characteristics of earthquakes and ground motion pertinent to the development of seismic input criteria are the size of the earthquake, the intensity and the frequency content of the ground motion, and the duration of strong shaking.

Size of earthquake

The size of the earthquake is typically represented for engineering purposes in terms of its magnitude. Several different magnitude scales are currently in use, the most common being the local magnitude, M_L; the surface wave magnitude, M_S; the body wave magnitude, M_B; and the moment magnitude, M_W. Definitions of each of these scales and their application are given by Housner and Jennings (1982). Physically, the magnitude has been correlated with the energy released by the earthquake, as well as the fault rupture length, felt area, and maximum displacement. Typically the magnitude is estimated, either in a deterministic or in a probabilistic manner, using general or site-specific correlations between the magnitude and the fault rupture length. The engineer will use the estimate of magnitude in conjunction with empirical attentuation relationships to define the intensity of the ground motion experienced at a specific site at some distance from the earthquake source.

Intensity of the ground motion

The intensity of the ground motion is obtained from recorded ground motion time histories. Several parameters, including peak acceleration, peak velocity, peak displacement, spectrum intensity, and root-mean-square acceleration are used; the most widely used measure is the peak ground acceleration. However, peak ground acceleration is not necessarily a good measure of damage potential because it is often repetitive shaking with strong energy content that leads to permanent deformation and damage. As a result, the term "effective

peak acceleration" has been used to refer to an acceleration which is less than the peak value but is more representative of the damage potential (Newmark and Hall 1982).

In view of the importance of predicting the ground motion that will be experienced at a particular site, considerable attention has been devoted to developing attenuation relationships based on correlations between field data on ground motion and the magnitude and distance of the earthquake. Ideally, such relationships should be established on a site-specific basis. In the absence of sufficient site data, use can be made of regional or global relationships such as given by Seed and Idriss (1982). When doing so, care must be taken to ensure that the correlation is based on data that is pertinent both in terms of geologic environment and the earthquake magnitude.

Frequency of content of the ground motion

The frequency content of the ground motion is commonly defined by a Fourier amplitude spectrum and/or a response spectrum. Both are obtained from computation of the response of a single-degree-of-freedom (SDOF) oscillator to base motion. The Fourier amplitude spectrum is a plot of the amplitude of the relative velocity for an undamped SDOF oscillator, at the end of a strong motion record, as a function of its frequency. It is less widely used for design purposes than the response spectrum, which is defined as a plot of the maximum response of a SDOF oscillator as a function of its frequency and damping.

The response spectrum, which is commonly plotted in logarithmic, tripartite form, derives its popularity from the fact that the SDOF oscillator is a reasonably good analogue for representing the significant response of many surface structures. This analogy does not hold for underground structures because they tend to move with the ground mass instead of vibrating independently. Hence, response spectra are generally less important to the designer of underground structures. However, they have application in the design of light structures located within an underground excavation. Also, the response spectra can be used to define the frequency content of a time-history input for a numerical simulation of ground/structure response, and for approximate definition of the peak ground motion parameters.

Duration of strong motion

The duration of strong motion can have a profound effect on the extent of damage resulting from an earthquake. In particular, it is reasonable to suppose that the number of excursions into the nonlinear range experienced by an underground structure and the surrounding media will control the extent of permanent deformation. Unfortunately, there is at present no universally accepted method of quantifying the duration of the ground motion; and the effects of repeated, cyclical loading on the performance of underground structures are very poorly understood. Until such understanding can be gained through detailed field investigations or numerical simulations, the designer should ensure that any empirically based design criteria are based on the performance of structures subjected to comparable loading, in terms of peak amplitude, frequency content, and duration.

Seismic Input Criteria

Several alternative approaches can be used for defining seismic input criteria. One approach involves the use of response spectra. This approach, which is the most widely used for surface structures, is covered in Appendix A. Another approach is to specify ground motion time histories. In this case an ensemble of motion time histories, rather than a single time history, should be specified. The family of motions should have the same overall intensity and frequency content, and should be representative of the anticipated shaking at the site due to all the significant potential earthquake sources in the vicinity of the site. The procedure used to select the motion time histories is described by Werner (1985).

An alternative approach for specifying seismic input criteria involves the use of seismic regionalization maps of the type used in current design codes and particularly in the seismic design guidelines suggested by the Applied Technology Council (ATC 1978). This approach is covered below.

Seismic regionalization maps

Seismic regionalization maps are intended to provide representative intensities of shaking for the regions under consideration, based on their seismologic and geologic characteristics. This intensity factor is used, together with a numerical factor that represents local site effects, in order to incorporate the influence of the seismic environment in the computation of equivalent forces upon which the seismic design of the structure is based (Berg 1982).

Although many seismic regionalization maps have been developed through the years, the maps included in the design provisions recommended by the Applied Technology Council (ATC-3) are the most current (ATC 1978). These maps, which are generally based on work by Algermissen and Perkins (1976), were developed using probabilistic procedures incorporating (1) identification of significant earthquake sources; (2) assessment of maximum credible magnitudes and magnitude-recurrence laws for each source; and (3) attenuation laws describing the intensity of shaking as a function of magnitude and distance from an epicenter. Based on the above principles, contours of locations with equal probabilities of receiving specific intensities of ground shaking are produced.

Two seismic regionalization maps provided in ATC-3 are reproduced in Fig. 1: one corresponds to "effective peak acceleration (EPA)," and the other to "effective peak velocity (EPV)." Neither of these parameters has precise physical definitions; however, a conceptual description of their significance can be found in the commentary of ATC-3 (1978). Although the EPA and EPV are related to peak ground acceleration and peak ground velocity, they are not necessarily the same as or even proportional to peak acceleration and velocity. The EPA expressed in units of g's (A_a) is used in ATC-3 to scale the intensity of the spectrum shape to obtain a design spectrum. The EPV expressed as a velocity-related acceleration in g's (A_v) is used (1) to adjust the spectrum shape to account for extended distance; and (2) to represent the strength of shaking in the computation of equivalent design forces.

Observed Effects of Seismic Loading of Underground Structures

Effects of Earthquakes

The previous section provided a general introduction to the subject of the dynamic environment associated with earthquakes. Our understanding of how surface structures, such as buildings, dams, or soil slopes, respond to such an environment has developed through observations made both during and after earthquakes. Early understanding of how to construct earthquake-resistant structures was based purely on qualitative observation. More recently, measurement and analysis have been used as the basis for development of improved design procedures.

A similar developmental process is occurring for underground structures, but the process is far from complete at present.

This section begins to follow the path of that development by reviewing the data on performance of underground structures. This material has been drawn primarily from reports of the effects of earthquakes, but some attention also will be devoted to relevant experience of the performance of excavations close to large underground explosions.

Damage Mechanisms

The effects of earthquakes on tunnels, mines, and other large underground

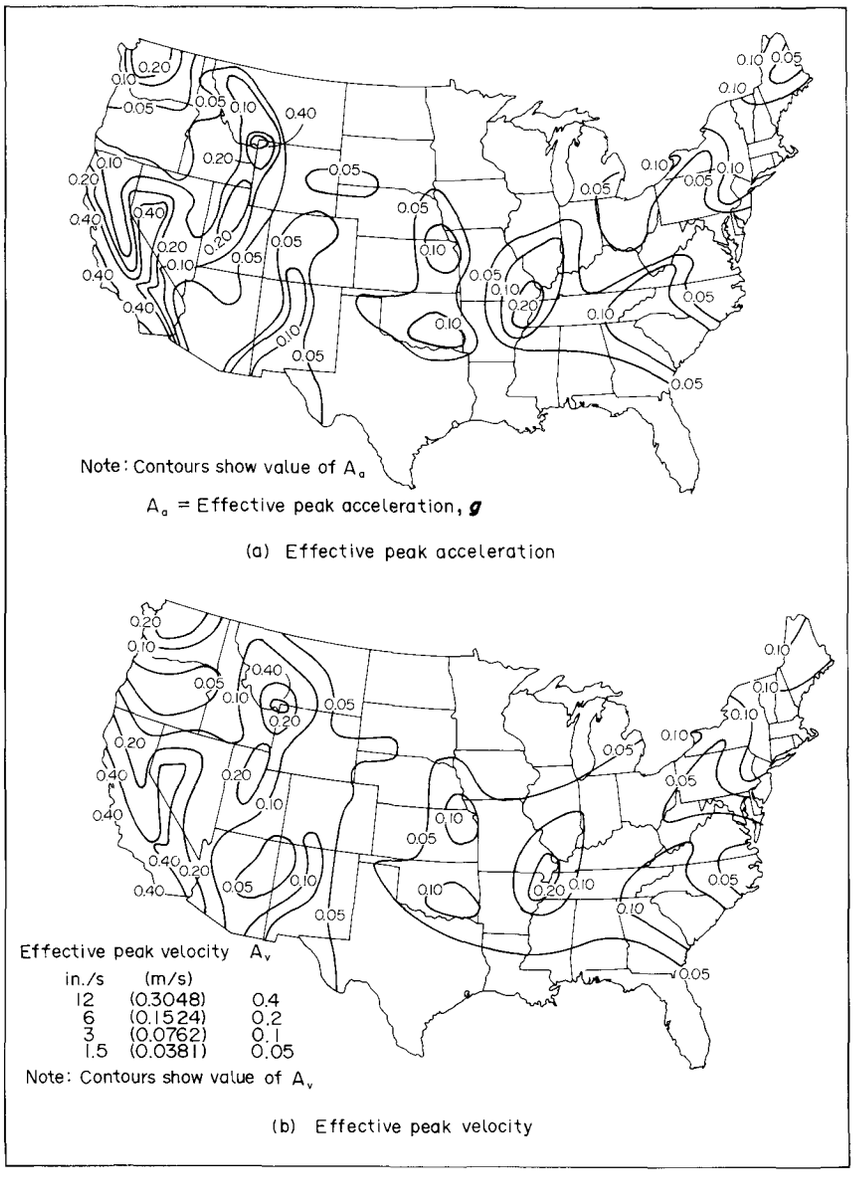

Figure 1. ATC-3 (1978) seismic regionalization maps.

excavations have been the subject of several reports. A comprehensive review of those reports and compilation of readily available data was prepared recently by URS/Blume and Associates on behalf of the National Science Foundation and the Federal Highway Administration Department of Transportation (Owen and Scholl 1981). In their review, earthquake damage to underground excavations was attributed to three factors:

- Fault slip.
- Ground failure.
- Shaking.

Damage due to fault slip occurs when the excavation passes through a fault zone. Under such circumstances damage generally is restricted to the fault zone, and may range from minor cracking of a tunnel liner to complete collapse, depending on the fault displacement and the engineering properties of the medium within which the excavation is constructed. Quite obviously, fault slip cannot be prevented. Hence, if an excavation crosses an active or potentially active fault zone, special design/planning measures should be prepared. Either the underground excavation and its support system must be designed to accommodate that displacement without loss of utility, or post-earthquake repair plans and emergency safety-related plans should be developed in advance.

Damage attributed to ground failure may be associated with rock or soil slides, liquefaction, soil subsidence, and other phenomena that may be triggered by ground motion. This type of damage is particularly prevalent at portals and in shallow excavations, and is not covered in this report. Suffice it to say that the potential for occurrence of this type of damage should be evaluated through particularly careful site investigation in the vicinity of tunnel portals and other underground shallow excavations.

Damage caused by shaking or vibratory motion has been most widely investigated and is the major topic of this report. For lined tunnels, damage may include cracking, spalling, and failure of the liner as a direct consequence of the shaking. Alternatively, vibratory motion may reduce the strength of the ground, thereby placing additional loads on the tunnel support system. For unlined underground excavations in rock, such damage occurs as rock fall, spalling, local opening of rock joints, and block motion.

Naturally, the response of any underground excavation to earthquake shaking will be influenced by many variables. The more important of these are the shape, dimensions, and depth of the excavation, the properties of the soil or rock within which the excavation is constructed, the properties of any support system, and the severity of the ground shaking. Summaries of the performance of underground excavations during earthquakes should account for all these variables. Unfortunately, much of the data essential for detailed analysis of damage experienced during an earthquake are often unobtainable. Accordingly, investigators of the performance of underground excavations have attempted to develop direct empirical relationships between damage levels and ground motion parameters. Such attempts are fraught with difficulties since damage assessments may be highly subjective and the peak ground motion experienced at a site must often be deduced from very incomplete data. Therefore, it is desirable that arrays of strong instruments be deployed in and around important underground structures.

The empirical data base

The first step in developing an empirical damage model is to define the various levels of damage to be considered. Dowding and Rozen (1978) identified three levels of damage for underground excavations in rock due to ground shaking: these were no damage, minor damage, and damage. *No damage* meant no new cracks or falls of rocks; *minor damage* meant new cracking and minor rockfalls; and *damage* included severe cracking, major rockfalls, and closure.

Dowding and Rozen presented results of correlation of the estimated peak surface acceleration and peak particle velocity with reported damage. Their correlations are reproduced in Figs 2 and 3. The numbers on the ordinate axis are the designations of the cases tabulated in their paper. The same numbering system also is used within the extensive tabulation of damage prepared by Owen and Scholl (1981). It should be noted that the peak ground motion parameters (acceleration and

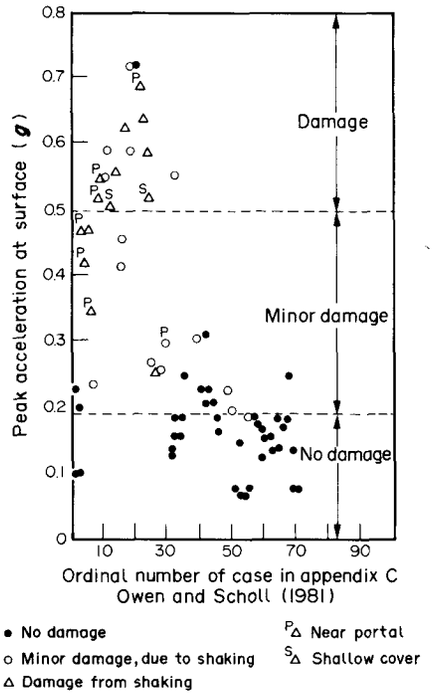

Figure 2. Calculated peak surface accelerations and associated damage observations for earthquakes (Owen and Scholl 1981).

velocity) were not recorded at the sites of the excavations but were calculated using empirical relationships such as those described in Appendix A. Strong motion mesurements from instruments placed in and around tunnels could provide much more reliable data in the future.

Review of data such as those presented by Dowding and Rozen suggests that no damage should be expected if the peak surface accelerations are less than about 0.2 ***g***, and only minor damage should be experienced between 0.2 and 0.4 ***g***. The corresponding thresholds for peak particle velocity are approximately 20 cm/s (8 in./s) and 40 cm/s (16 in./s). Of these two correlations, the one based on velocity is probably to be preferred as a design criterion because the peak particle velocity resulting from an earthquake of a given magnitude can be predicted to fall within reasonably narrow limits. Moreover, experience on the performance of mining excavations adjacent to rock bursts has indicated that damage is better correlated with peak velocity than peak acceleration (McGarr 1983).

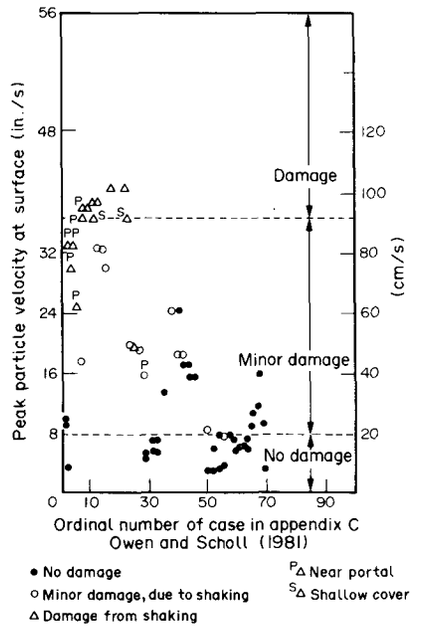

Figure 3. Calculated peak particle velocities and associated damage observations for earthquakes (Owen and Scholl 1981).

It should be emphasized that the above relationships hold for rock sites only, and may be very different for underground structures in soil because the attenuation of motion with depth and the confinement of the structure are very different than those for rock sites. Unfortunately, similar relationships have not yet been derived for underground structures in soil.

Supporting evidence

Supporting evidence for selection of an empirical design criterion for rock sites is provided from experience in the mining industry, civil construction involving blasting, and weapons testing. As alluded to above, there are a number of cases in which underground mining excavations have been damaged as a consequence of nearby rock bursts. The best documented cases are for the deep level gold mines of South Africa, where rock bursts with body wave magnitudes up to 5.2 have been triggered as a result of extensive longwall mining of the tabular gold reefs. Whether any damage accompanies a rock burst depends on the magnitude of the event and its proximity to the mine workings. Experience indicates that rock bursts with energy release corresponding to up to a 2-2.75 magnitude earthquake occasionally cause damage if they are associated with a major rupture within about 30 m of the mine workings. Events of larger magnitude are almost invariably damaging enough to cause loss of production and, possibly, injuries or fatalities, providing they are sufficiently close to mine workings to generate velocities in excess of 60 cm/s (24 in./s).

Because rock bursts are similar in character to tectonic earthquakes (although the resulting duration of shaking typically is much shorter), the records of damage to mining excavations provide direct evidence of the likely performance of excavations very close to a causative fault. How pertinent the experience is to the performance of excavations remote from the source of an earthquake depends upon how important a role the duration and dominant frequency of the ground motion play in determining the extent of damage. If the frequency content is relatively unimportant, then the experience gained in the mining industry is relevant. Further, data on the effects of ground motion induced by high explosives and nuclear weapons also are of value. For the present, we shall defer any discussion of the importance of duration and frequency content and simply summarize the empirical data base.

The requirement to minimize the damage to underground tunnels due to conventional blasting has led to development of empirical design criteria. For unlined tunnels in rock, Langefors and Kihlstrom (1963) suggest that particle velocities of 30 cm/s (12 in./s) cause rock to fall while velocities of 60 cm/s (24 in./s) cause the formation of new cracks in the rock. These recommendations seem rather conservative when compared with the results of the Underground Explosion Test Program (UET), during which very large charges of high explosives were detonated with the intent of establishing design criteria for construction of underground installations. Damage, consisting of intermittent spalling, was observed for particle velocities above 90 cm/s (36 in./s). Continuous damage was observed for particle velocities above 180 cm/s (72 in./s).

Since the UET high explosive tests, several tunnel test sections have been included within the scope of underground nuclear tests. Although most of the tunnel sections have been hardened, using various types of concrete and steel liners, some have been supported only with rockbolts and light shotcreting. Review of the performance of all those sections indicates that tunnels hardened with rockbolts may survive peak particle velocities in excess of 900 cm/s (360 in./s) but the threshold for damage to unlined tunnels is on the order of 180 cm/s (72 in./s).

These values are so far in excess of anything that could conveivably result from an earthquake that one is tempted to dismiss the problem of seismic stability of deep underground excavations as trivial. However, there is one important difference between the ground motion resulting from an earthquake and that generated by a nuclear explosion. The former usually lasts for several seconds, subjecting the excavation to several stress cycles, while the latter predominantly comprises a single pulse (compression) lasting some tens to hundreds of milliseconds. The results of numerical experiments reported by Dowding et al. (1983) suggest that the number of stress cycles is critical to determining how much permanent deformation will occur within a rock mass around a tunnel when it is subjected to earthquake loading.

Conclusions

The results of attempts to catalogue

records of the performance of underground excavations subjected to seismic loading and to develop simple empirical design criteria indicate a damage threshold of approximately 20 cm/s (8 in./s). No damage should be experienced if the peak particle velocity is beneath that threshold. This threshold is valid for underground structures in rock and may not be applicable for other types of excavations. Although there are important differences between the ground motion resulting from large distant earthquakes and rock bursts, detonation of high explosives, or nuclear explosions, data from these sources provide supporting evidence that adoption of this threshold value as a design criterion will be conservative. It can be expected that this recommended damage threshold will be raised as more data becomes available.

Models of the Seismic Response of Underground Excavations

Once design progresses beyond the application of simple empirical relationships, such as those described in the previous section, models become an integral part of the design process. Selection of the appropriate model must be made by the designer on the basis of the type and importance of the structure being designed and the quality of the available or obtainable geotechnical data. Early selection is to be encouraged, as the model may have data needs that must be satisfied during site investigation.

This section provides a brief review of the analytical tools available to the designer concerned with the performance of underground excavations subject to seismic loads. The analytical tools form the basis of more or less complicated numerical models of the behavior of geologic media and interactions between geologic media and underground structures. The review starts with a brief discussion of analytical tools used to investigate relative displacements that occur along faults and other discontinuities in rock masses. Specific consideration is given to methods of evaluating the potential for displacement on faults and block motion. Subsequently, attention is devoted to the subject of wave propagation in geologic media and analytical tools for evaluating soil/structure interaction effects.

Relative Displacement Models

Brief mention of the need to design underground excavations, and any support systems, to withstand fault displacement was made in the previous section. Fault displacement, whether on the causative fault or triggered on some other fault, is one form of relative displacement. For convenience, we have chosen to differentiate this phenomenon from block motion or relative motion of rock mass in fractured media, which comprises the motion of some finite block of material relative to its surroundings. Although block motion may be triggered by earthquakes, it has been more widely investigated as a phenomenon associated with detonation of high explosives or nuclear weapons.

Fault displacement

Designers of surface structures are concerned with the surface manifestation of a causative fault. The designers of underground structures are also concerned with how that manifestation might change with depth. In the above discussion of seismic activity, little attention was given to either of these design considerations, although it was noted that one measure of the magnitude of an earthquake—the moment magnitude—is defined in terms of the total elastic strain-energy released and, therefore, is related to the fault displacement and rupture area. More specifically, the seismic moment is defined as

$$M_0 = GAD, \tag{1}$$

in which G is the shear modulus of the rock, A the area of the rupture surface, and D the average relative displacement (Kanamori and Anderson 1975). This relationship provides one means of estimating the average fault displacement, providing that the fault geometry is adequately defined. A better alternative is to use site-specific data.

Geodetic surveying of surface movements associated with large earthquakes has provided data on how displacements decay with distance from the fault. Unfortunately, there is much less data on the distribution of relative displacement on the fault plane. However, some insight has been gained through use of relatively simple numerical models in which the fault is modeled as a dislocation in a semi-infinite elastic medium. For example, Pratt et al. (1979) report the results of a series of simulations of strike slip and dip slip faults with various geometries. While it is difficult to draw general conclusions from the few cases they considered, their results did indicate that there may be circumstances in which the displacement of the medium adjacent to the fault may be greater at depth than on the surface. However, it is generally assumed that the relative displacement experienced underground is comparable to that experienced on the surface. This assumption can be checked quite easily for a particular fault geometry and boundary conditions using the displacement discontinuity method described by Crouch and Starfield (1983).

Relative displacements may be experienced on faults other than the causative fault. This may occur if the seismically induced stresses and the local *in-situ* stress conditions are such as to induce shear failure on the fault. Although qualitative predictions of such displacement using numerical models based on finite element or finite difference methods are possible in principal, lack of site data and the computational effort required militate against making such calculations.

As an alternative, the problem of incipient fault motion can be investigated using the simplified approach developed by Johnson and Schmitz (1976). Their model is based on calculating the shear and normal stresses, on a fault plane, that result from propagation of a spherical wave from a source. Conditions of incipient slip exist if the total shear stress (the sum of *in-situ* and induced stress) exceeds the shear strength. The model was originally developed to investigate fault movement induced by an explosion, which can be adequately represented as a spherical source. Although the spherical source is not a good idealization of an earthquake, the model still should provide a basis for establishing an understanding of the more critical fault orientations and locations.

Block motion

For excavations in fractured media, attention focuses on containing the fractured mass or individual blocks of material defined by pre-existing fractures. However, it is convenient to initiate the topic of analytical tools for design under such circumstances by first considering the topic of spalling—a phenomenon that may be induced by reflection of a stress wave at a free surface.

Interest in the performance of underground excavations in rock subjected to very high seismic loads, such as those induced in the vicinity of an underground weapons test, resulted in evaluation of spalling as a possible damage mechanism. Labreche (1983) used the results of work by Rinehart (1960) on the subject of spalling to interpret damage observed in tunnels adjacent to tests of both high explosives and nuclear weapons. He concluded that spalling due to tensile failure of the rock mass was unlikely, except very close to a high explosive detonation, because the spall thickness would be greater than the spacing of pre-existing fractures. On the other hand, pseudospalling, or separation along pre-existing fractures, appeared to be an important damage mechanism.

Rinehart (1960) showed that the pseudospall velocity will approach the free-field particle velocity for stress waves that have a very sharp front. For waveforms and wavelengths of concern

in the design of underground excavations subjected to earthquake loading, the pseudospall velocity is likely to be much less because the stress wave will have completely engulfed the excavation, thereby constraining the movement of potentially unstable blocks or slabs. Hence, simple spall models have very limited application in design against earthquake loading.

Because of the relative unimportance of the dynamic phenomena, including spalling or pseudospalling, it is conventional to treat the behavior of an excavation in fractured media as pseudostatic; this is the case for continuum modeling as well. However, in this case the primary concern is design against the possibility of separation of blocks of material from the surrounding medium. Blocks of ground that are kinematically capable of moving into the excavation are assumed to be accelerated differentially at the peak free-field ground acceleration. An approach to defining the shape, dimensions, and support requirements of such blocks is presented by Hoek and Brown (1981), who primarily make use of simple graphical constructions coupled with limiting equilibrium considerations. A more comprehensive approach to defining kinematically admissible blocks is provided by the keyblock theory developed by Goodman and Shi (1985). Some progress has been made in using this method, which enables all critical blocks to be identified, as a starting point for predicting support requirements (Goodman et al. 1982).

The alternative to attempting to identify blocks with particular geometric shapes is to rely more on precedent. For example, Barton (1981) has suggested modification of the Q system to account for seismic effects. Also, Hendron and Fernandez (1983) describe the application of Cording's (1971) method for prediction of the support pressures for the roofs of large underground excavations. They defined the required support pressure (p_i) for the roof of a cavern as

$$p_i = (1.0 + a/g)\, n\, B\, \gamma \qquad (2)$$

in which n is an empirically derived factor, B is the span of the cavern, γ is the unit weight of the material, a is the ground acceleration, and g is the acceleration due to gravity. This equation implies that details of the structure in the roof are relatively unimportant; a reasonable assumption, provided that compressive stresses in the roof are sufficient to inhibit slip along the relatively steep fractures that have a potential for defining blocks kinematically capable of differential movement.

The alternative to simple design models is to resort to more detailed simulation using one of the several available numerical modeling methods. The latter are relatively well developed for analysis under static and pseudostatic conditions, but have been applied only relatively recently to dynamic analysis of fractured media. Two fundamentally different approaches to modeling of fractured media have been adopted. One approach involves starting from a numerical procedure originally devised to describe the behavior of a continuum, while the other model approaches the problem as one of describing the behavior of a discontinuum.

One continuum approach involves using special interface elements, such as discussed by Goodman and St John (1977). This approach has the disadvantage that large shear displacements will necessitate repeated rezoning, or redefinition of the finite element mesh. Probably for that reason, the large deformation wave propagation codes such as HONDO (Key et al. 1978), DYNA2D (Hallquist 1978), and STEALTH2D (Hoffman 1981) more typically treat interfaces as slide lines between structurally independent components. Although this approach appears to have been used very successfully to study complex impact problems, its application to problems other than very simple layered geologic media appears to have been limited.

An alternative continuum approach relies on using special constitutive descriptions of a fractured media that account for the mechanical properties of the fractures and their spacing and orientation. The CAVS model that was used by Wahi et al. (1980) to investigate the stability of nuclear waste isolation caverns subjected to simulated earthquakes is an example of such a constitutive description. Such models readily permit the simulation of the development of new fractures within a particular element or zone, but do not explicitly represent the location of each fracture. Accordingly, the kinematics of block movement are ignored.

To overcome the difficulty in describing the kinematics of blocky systems, Cundall (1971a,b) developed the distinct element method. In that method, a fractured medium is viewed as an assembly of interacting particles which, in the most general implementations of the method, are completely free to move with respect to each other. In its earlier implementation, the blocks were considered to be rigid and infinitely strong; thereby restricting all deformations to the fractures and severely limiting possible failure modes. Recent generalizations of the approach allow deformable blocks and development of new fractures in addition to more comprehensive descriptions of the mechanical behavior of the fractures (Cundall and Hart 1983).

Although the distinct element method is based on the equations of motion of the individual particles, it has been most widely applied to the solution of pseudostatic problems by treating time as a fictitious quantity used to control the sequence of events in a system that may exhibit complex nonlinear behavior. However, it is equally possible to perform dynamic analyses.

Such an approach is described by Dowding et al. (1983) who report the application of a coupled distinct element/finite element model in an investigation of the response of a cavern to vertically propagating shear waves. One of the most interesting aspects of their investigation was the extent to which ground motion resulted in progressive slip on the faces of blocks adjacent to the excavation. However, extremely high accelerations were required for this to occur. Continuing development of the distinct element method for dynamic analyses, coupled with studies such as described by Dowding et al., will undoubtedly contribute significantly to our understanding of the basic mechanics of fractured media.

Vibratory Motion

Although most of the relative displacement effects discussed above result from wave propagation from the source through geologic media, it proves convenient to discuss the direct effects of vibratory motion as a separate subject. This discussion is divided into two main parts. The first part considers the ground motion in the free field, with particular attention given to how the ground motion is influenced by the geologic structure. The second part considers how underground structures respond to vibratory motion. The latter discussion is subdivided into three parts. First, results of analyses of lined and unlined circular tunnels in elastic media are summarized. Second, the bases for development of simple models for investigating ground structure interaction effects are discussed. Third, the capabilities of numerical models that may be used to investigate ground/structure interaction effects in greater detail are reviewed.

Free-field ground motion

The problem of free-field ground motion, also known as wave propagation, in an infinite homogeneous isotropic elastic medium was addressed as early as 1950 (Fung 1965; Desai and Christian 1977). This section describes the formulation and solution of the three-dimensional wave equations and the depth dependence of ground motion.

The motion of a continuum body must obey the equation

$$\rho\, \alpha_i = \frac{\partial \sigma_{ij}}{\partial x_j} + X_i \qquad i = 1, 2, 3 \qquad (3)$$

where ρ = mass density of the continuum,
α_i = particle acceleration,
σ_{ij} = stress field, and
X_i = body force per unit volume.

In the theory of elasticity, the above equation is known as the Eulerian equation of motion of a continuum. If we limit ourselves to the linear theory or infinitesimal displacement theory, we can write the following relationships between strain, e_{ij}; particle displacement, u_i; particle velocity, v_i; and particle acceleration, α_i:

$$e_{ij} = \frac{1}{2}(u_{i,j} + u_{j,i}) \tag{4}$$

$$v_i = \frac{\partial u_i}{\partial t}, \quad \alpha_i = \frac{\partial v_i}{\partial t} = \frac{\partial^2 u_i}{\partial t^2} \cdot \tag{5}$$

In addition to the above equations, the theory of linear elasticity is based on Hooke's law. For a homogeneous isotropic material, this is

$$\sigma_{ij} = \lambda\, e_{kk}\, \delta_{ij} + 2G\, e_{ij} \tag{6}$$

where λ and G are called Lame's constants. The stress field σ_{ij} can be eliminated by substituting Equation (6) into Equation (3) and using Equation (4) to obtain the well-known Navier's equation

$$G\, u_{i,jj} + (\lambda + G)\, u_{j,ji} + X_i = \rho \frac{\partial^2 u_i}{\partial t^2}. \tag{7}$$

The above equation can be cast in different forms and its general solution for the case of a steady state harmonic motion can be easily calculated (Achenbach 1975). In the next section some types of waves that satisfy the above equation of motion are considered.

Plane elastic waves

Several types of waves can propagate in an elastic medium. Their existence can be demonstrated from the basic field equation (Equation (7)), which, in the absence of body force, is

$$\rho \frac{\partial^2 u_i}{\partial t^2} = G\, u_{i,jj} + (\lambda + G)\, u_{j,ji} \cdot \tag{8}$$

In the following discussion, displacement components u_1, u_2, u_3 will be referred to by u, v, and w; they represent, respectively, the motion parallel to the direction of wave propagation, the motion in the horizontal plane normal to the direction of wave propagation, and the motion in the vertical plane normal to the direction of wave propagation.

One type of particle motion can be defined by

$$u = A \sin \frac{2\pi}{L}(x \pm ct), \tag{9}$$

$$v = w = 0 \cdot$$

Substitution of Equations (4-9) into the field equation, leads to the relationship

$$\rho\, C_p^2 = \lambda + 2G \tag{10}$$

or

$$C_P = \sqrt{\frac{\lambda + 2G}{\rho}} \cdot \tag{11}$$

where C_p has been substituted for c and represents the wave velocity. The pattern of motion expressed by Equation (9) remains unchanged when $(x \pm ct)$ remains constant and L is the wavelength. The particle velocity is in the direction of propagation, namely the x-direction. Hence, this motion is said to represent a compressional wave or P-wave.

A second type of motion can be defined by

$$u = 0$$

$$v = A \sin \frac{2\pi}{L}(x \pm ct) \tag{12}$$

$$w = 0$$

which represents a train of plane waves of wavelength L propagating in the x-direction with a velocity c. The substitution of Equation (12) into the field equation yields a value for the wave velocity, C_S, given by

$$C_S = \sqrt{\frac{G}{\rho}} \cdot \tag{13}$$

The particle velocity is in the y-direction and is perpendicular to the direction of propagation, namely the x-direction. Such a motion is said to represent transverse or shear waves (S-waves).

A third type of motion, which represents transverse waves can also be defined by

$$u = 0$$

$$v = 0 \tag{14}$$

$$w = A \sin \frac{2\pi}{L}(x \pm C_S t) \cdot$$

This wave is similar to the previous wave except that the particle motion is in the z-direction. In order to differentiate between the two motions, one is referred to as transverse horizontal (SH), and the other as transverse vertical (SV), depending on whether the wave is propagating in a horizontal or a vertical plane, respectively.

For all of the above waves, the motion represented by Equations (9), (12) and (14) are called plane waves, since at any instant of time the wave crests lie in parallel planes. These waves may exist only in an unbounded elastic continuum. In a finite body, a plane wave will be reflected when it hits the boundary. If there is another elastic medium beyond the boundary, refracted waves occur in the second medium. The problem of reflection and refraction is addressed below.

Of course, arbitrarily incident plane waves can propagate within a medium. For these waves, the governing equations of motion can be found elsewhere (Achenbach 1975).

Surface waves

In addition to the waves that propagate within an elastic medium, i.e. body waves, it is possible to have another type of waves—that is, those that propagate over the surface of the medium and penetrate to only a minor extent into the interior of the body. These are called surface waves. For these types of waves, it is characteristic that the amplitude of displacement in the medium decreases exponentially with increasing distance from the boundary.

One type of surface wave is the Rayleigh wave, which occurs on the free surface of a homogeneous, isotropic, semi-infinite medium. In a two-dimensional elastic half-space with $y \geq 0$ and a stress-free surface at $y = 0$, the motion can be defined by the real part of the following expressions

$$u = A\, e^{-by} \exp[ik(x - ct)]$$

$$v = B\, e^{-by} \exp[ik(x - ct)] \tag{15}$$

$$w = 0$$

where i is the imaginary number $\sqrt{-1}$, and A and B are complex constants. The coefficient b is considered to be a real and positive constant so that the amplitude of the wave decreases exponentially with increasing y, and tends to zero as y approaches infinity. The constants in the above expressions are chosen such that the displacement equations satisfy the equations of motion and the boundary conditions on the free surface.

The proof of the existence of Rayleigh waves can be found in books on classical theory of elasticity (Fung 1965), and is not repeated here. However, an illustration of the elliptical retrograde-type motion and a discusion of the relative propagation velocities of compressional, shear and Rayleigh waves are included within Appendix A. The illustration shows that for the Rayleigh waves the particle motion is in the plane of wave

propagation. Surface waves with motion perpendicular to the direction of propagation can occur if the shear wave velocity in the upper layer is less than that in the lower stratum. These waves are known as Love waves. Again, the equations of motion governing these types of waves can be derived analytically (Achenbach 1975).

Reflection and refraction of plane waves

To illustrate the problem of reflection and refraction of plane P and S waves, consider a homogeneous isotropic elastic medium occupying a half space and with a free surface. Plane P waves hitting the free boundary are reflected into the medium as plane P waves and plane S waves. Similarly incident SV waves are reflected as both P and SV waves.

If the medium consists of two or more layers, then incident P waves propagating in one layer are reflected into P and SV waves and refracted into the adjacent layer as P and SV waves. The same holds for incident SV waves. The SH waves behave differently. A train of SH waves will not generate P waves at the interface; it is reflected and refracted as SH waves.

Amplification of SH waves

Body and surface waves are created by disturbances caused by an earthquake. The amplitude and frequency content of the earthquake motion depend on the source and the transmission path as well as site characteristics. Along the transmission path, body waves are influenced by the geometry and material properties of the medium. They are reflected and refracted between layers of different material properties—a phenomenon that results in a local decrease or increase of the wave amplitude and affects the frequency content of the resulting motions.

For the practicing engineer, the problem is to determine the characteristics of the ground motion at a site (surface and/or underground motion) on the basis of the motion recorded at other sites. In view of the complexity of the waves propagation problem, it is not possible at present to solve the general problem, which includes body waves (P- and S-waves) and surface waves. Therefore, consideration has been restricted here to the case of vertical propagation of horizontally polarized shear waves in a horizontally layered medium—a case for which an analytical solution can be easily derived using one-dimensional wave theory. While this approximation has its limitations in representing the actual problem, it is based in part on the observation that body waves reaching the site from the source of the disturbance arrive, in general, with nearly vertical incidence to the ground surface, and not in a straight line from the source to the site (Tsai and Housner 1970).

A continuum solution to the one-dimensional wave equation can be used to analyze the free-field response of a horizontally layered site subjected to vertically incident shear waves. The analysis is carried out in the frequency domain by utilizing the Fourier Transform of the input motion to represent the motion as the superposition of harmonic signals of different frequencies. The frequency-dependent transfer function of the system is obtained by computing the response of the system to unit harmonic input motion. The time-dependent system response to the actual input motion is then obtained as the inverse Fourier Transform of the product of the system transfer functions and the various harmonic signals that comprise the input motion. The above procedure is carried out when the motion is defined at the base of the soil layers. A deconvolution procedure can be used to compute the subsurface motion once the surface motion is defined.

The theoretical derivation of the equations for the above procedure are involved and beyond the scope of this report. They can be found in Desai and Christian (1977). The result of this exercise is to define the amplification factor or the ratio of the amplitude of motion at the free surface to the amplitude of motion at rock/soil interface. A typical shape for the amplification factor of a uniform soil layer above rock is shown in Fig. 4. For other cases computer programs such as FLUSH (Lysmer et al. 1975) and SHAKE (Schnabel et al. 1972), which are based on the above procedure, can be used. These codes are discussed below.

Seismic analysis of underground structures

A wide range of analytical tools has been used to investigate the behavior of underground excavations subjected to seismic loading. Because they can be analysed in closed form, particular attention has been devoted to analysis of lined and unlined circular tunnels. The emphasis of that work has been on investigating the results of plane waves propagating perpendicular to the longitudinal axis of the tunnel. For the case of waves propagating along the axis, use has been made of simplified models in which the tunnel liner is idealized as a beam on an elastic foundation.

More recently, attention has turned towards the use of a number of different numerical procedures that enable ground/structure interaction problems to be studied in either the time domain or frequency domain. The following discussion comprises a brief review of these three areas of investigation.

Circular and noncircular tunnels

A considerable body of literature is devoted to the development and application of analytical solutions to the problem of plane waves propagating in an elastic medium; normal to a tunnel axis. Interaction of the wave and the tunnel causes a distortion of the cross-sectional shape and stress concentrations over and above those resulting from the *in-situ* stresses existing prior to excavation. Interaction can also take the form of entrapment and

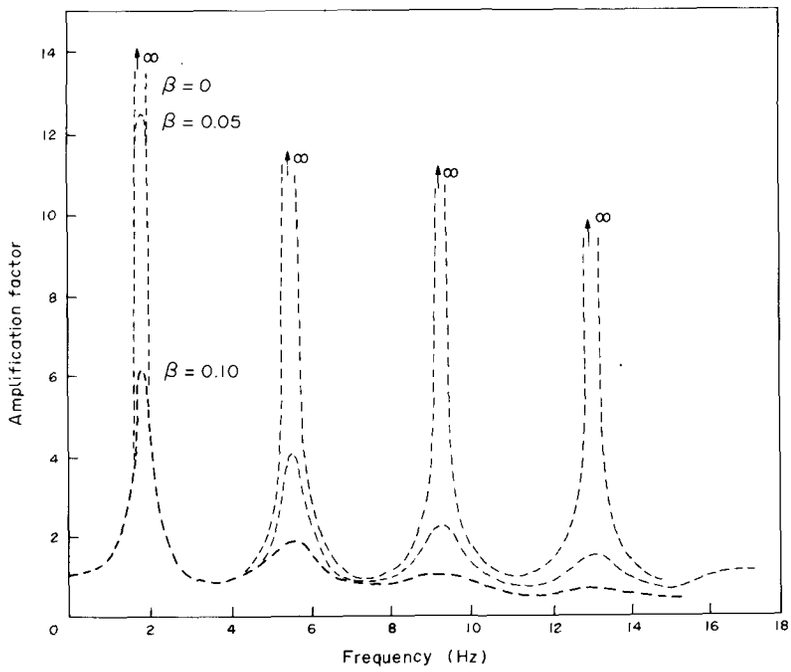

Figure 4. Amplification curve for uniform layer with rigid rock (modified from Desai and Christian 1977).

circulation of the seismic waves around the tunnel. However, this is only possible when wavelengths are less than the tunnel's radius (Glass 1976) and the circulating waves appear to be heavily damped because they radiate energy into the solid (Cundall 1971a,b).

Using closed-form solutions, Mow and Pao (1971) investigated the interaction of steady state P-, SV-, and SH-waves with cylindrical cavities. For P-waves propagating normal to the longitudinal axis, they demonstrated that the peak dynamic stress concentrations were approx. 10–15% higher than those resulting from static stress equal to the peak free-field stress; and that these stress concentrations occur for wavelengths that are approx. 25 times the cavity diameter. The stress concentrations resulting from SV- and SH-waves also were a few percent higher than the static equivalent. The importance of these results is not so much that the dynamic effects are small, but that static or pseudostatic analyses are adequate for wavelengths typically associated with earthquake-induced ground motion.

Results presented by Mow and Pao indicated that there will be very little concentration of stress if the wavelength is short in comparison to the diameter of the cavity. Such short wavelengths are unlikely to be important for earthquake loading, except very near to the source, but can be important for excavations subjected to loading from conventional or nuclear explosions. For very short wavelengths, the wall of the excavation acts like a plane-free surface at which the stress wave is reflected as a wave of opposite sign. Hence, incoming compression wave induce, upon reflection, tensile stresses and create stress concentrations that interact with the reflection. The presence of tensile stresses raises the possibility of spalling (a phenomenon that has been covered above).

The real problem of spalling at underground excavations is more complex than was considered by Rinehart, since the incoming stress creates stress concentrations that interact with the reflection. The problem of interaction can be investigated quite simply in closed form. Typical results from a number of recent calculations using a computer code developed by Garnet et al. (1966) are reproduced in Figs 5 and 6, in which the relationship between time, stress, and distance from the tunnel wall is illustrated for the case of a triangular plane P-wave engulfing the opening. The total duration of the waveform is equal to the travel time across eleven tunnel diameters, with the stress rising linearly to a peak in one tunnel diameter. At time zero, the wave has just reached the wall of the tunnel; its front can be seen clearly in Fig. 5. The front is indeed reflected; however, if

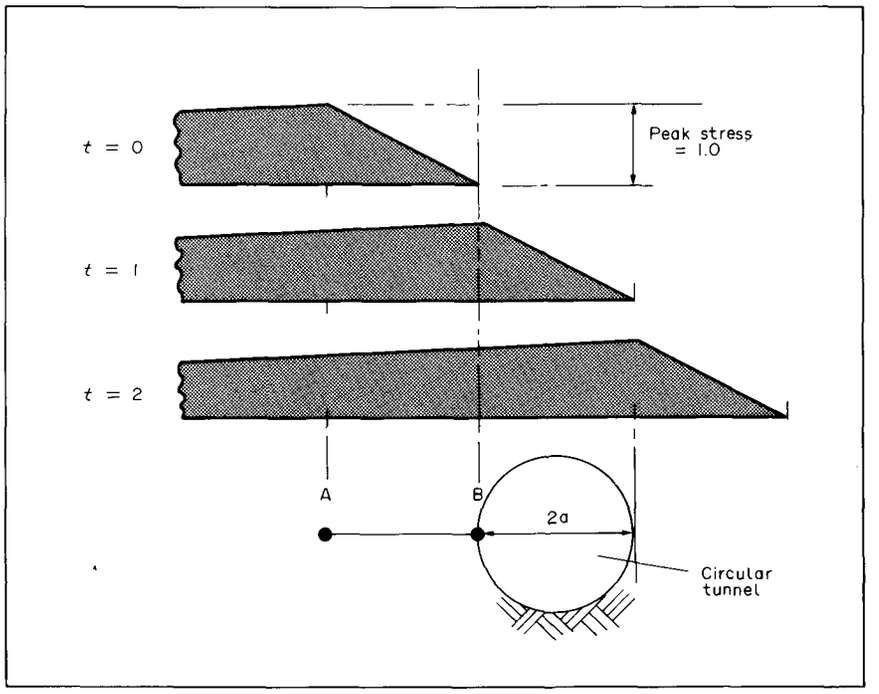

Figure 5. A triangular wave with wavefront and total length equal to one tunnel diameter and eleven tunnel diameters, respectively.

the wavelength is greater than about ten tunnel diameters, the induced radial stress remains compressive. Although Fig. 6a indicates that the induced hoop stress is tensile, this is to be expected since the P-wave induces a biaxial stress state in which the peak confining stress is related to the peak stress by the factor $\nu/(1-\nu)$.

The case of lined circular tunnels can also be analysed in closed form. Results comparable to those for the unlined tunnel are reproduced in Fig. 6b. What is noticeable in these figures is that there is a minor increase in the radial stress in the rock and a marked concentration of hoop stress in the liner. This is observed because the liner properties were chosen so as to make the liner appear stiff relative to the rock medium. Whether a liner will significantly interact with the medium depends upon the compressibility ratio and the flexibility ratio (Hendron and Fernandez 1983). Of these, the flexibility ratio is the more important because it is related to the ability of the liner to resist distortion.

The flexibility ratio, F, is defined by

$$F = \frac{2E\,(1-\nu_l^2)\,R^3}{E_l\,(1+\nu)\,t^3}$$

in which E and ν are the Young's modulus and Poisson's ratio of the medium and E_l, ν_l, R, and t are, respectively, the Young's modulus, Poisson's ratio, radius, and thickness of the liner.

Several investigators have discussed the relationship between the flexibility ratio and the extent to which a liner modifies a tunnel response to either static or dynamic loads (for example, Peck et al. 1972; and Einstein and Schwartz 1979). They concluded that the liner can be considered perfectly flexible if the flexibility ratio exceeds 20. In that case the liner conforms to the distortions imposed on it by the medium. If, on the other hand, the flexibility ratio is low, then the liner will resist the distortion of the medium. Whether there is a concentration of stress in the liner depends mainly on the relative elastic modulus of the liner and medium.

For the case illustrated in Fig. 6b the elastic modulus of the liner is twice that of the medium. However, the liner has a very high flexibility ratio (approx. 1000). Accordingly, the distortion of the medium is substantially unrestrained. In general, it would be conservative to check that the liner is capable of withstanding the unrestrained distortion of the medium.

Several closed-form solutions are available for estimating ground/structure interaction for circular tunnels. The solutions more commonly used for static design of tunnel liners have been reviewed by Duddeck and Erdmann (1982). They are based on the assumption that the liner behaves as a thin shell. In fact, the more general solution of a concentric elastic ring of any thickness can be derived quite simply; the necessary equations for the dynamic case are given by Garnet et al. (1966). Use of the static solution should be perfectly acceptable for evaluating the response to wavelengths typically associated with earthquakes, particularly if the static overstress is increased

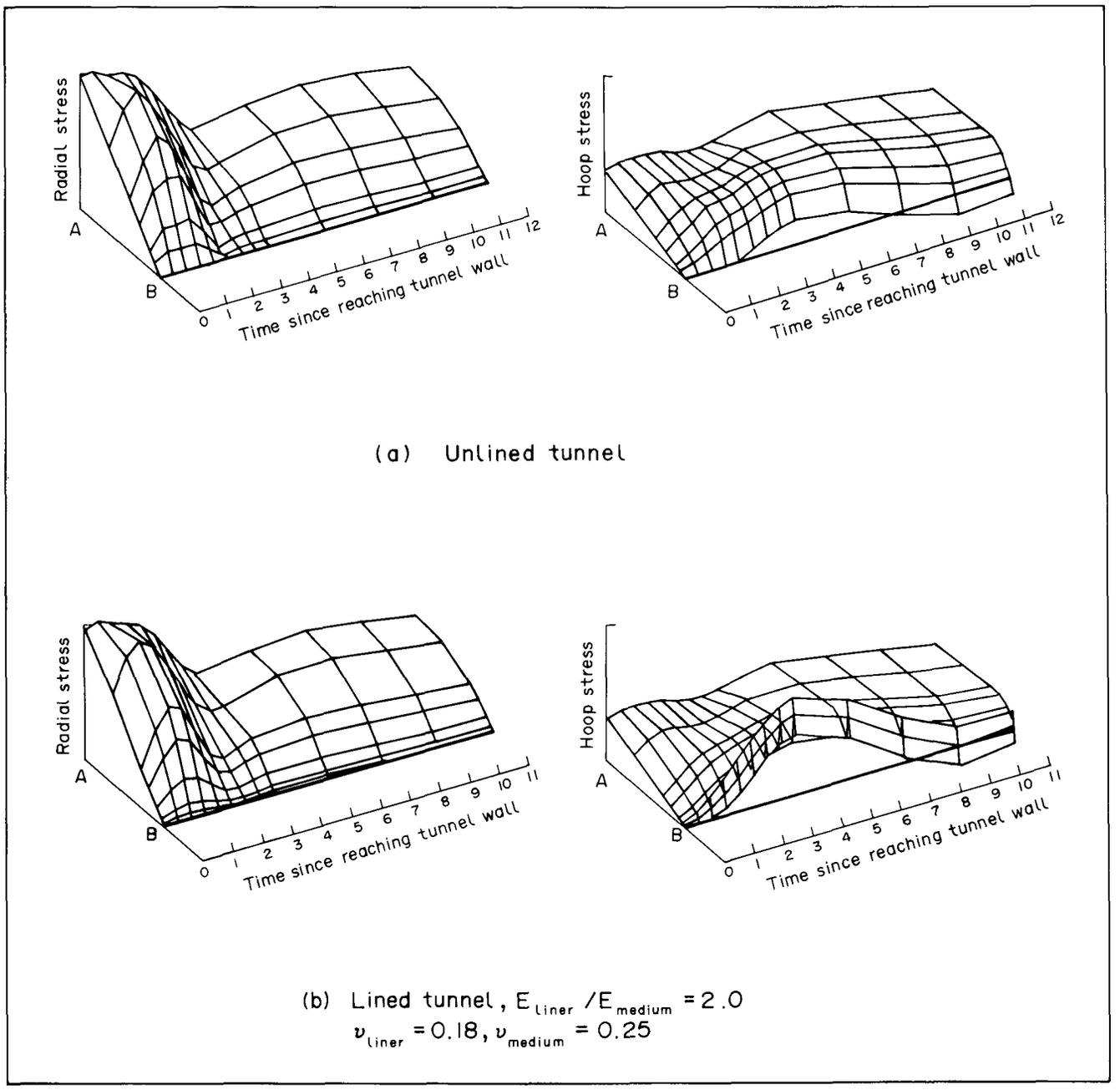

Figure 6. Radial and circumferential hoop stress histories in the wall of an unlined tunnel (a) and a lined tunnel (b). The stress profiles are for the line AB in Fig. 5.

10–15% above the peak dynamic free-field stress.

A note of caution in regard to the use of any of the lined tunnel solutions is in order. As O'Roark et al. (1984) point out, there are differences between the case of external loading of a lined tunnel and emplacement of a liner in a previously stressed medium. Providing the surrounding medium remains elastic, the liner stresses immediately after installation can be conservatively estimated by assuming that the processes of excavation and liner installation occur simultaneously. In practice, the liner is frequently installed after at least 50% of the elastic displacement of the medium has already taken place and the liner loads are correspondingly lower.

To evaluate the effect of earthquake loading, the solution for external loading should be used. Since both medium and liner are assumed to be linearly elastic, the post-excavation and earthquake-induced stresses, or thrusts and bending moments, can be superimposed to estimate the total loads. Remember, however, that the earthquake loading is cyclic and that the designer is concerned with the states of liner and medium at both extremes of the cycle.

Because of the availability of relatively simple closed-form analytical solutions for lined and unlined circular tunnels, the conditions resulting from plane wave propagating normal or near-normal to the tunnel axis are relatively well understood. Much less attention has been devoted to investigating the behavior of excavations, supported or unsupported, of different shapes. However, the general conclusions reached for the circular tunnels should be applicable.

Most importantly, we expect the response to earthquake loading to be near enough pseudostatic and we expect ground/structure interaction effects to be relatively unimportant providing the ground support system is relatively flexible. In practice, the ground support is generally flexible and the conservative approach of assuming that the liner experiences the unrestrained deformation of the medium can be adopted. If this approach results in the conclusion that special provisions need to be made to provide adequate safety, then it would be appropriate to conduct more

thorough ground/structure interaction calculations using one of the numerical modeling tools discussed below.

Simple ground structure interaction models

If the flexibility ratio of a liner, as defined above, is low, then the liner is stiff compared to the medium and will resist the distortions imposed on it by the medium. Of course, it will be conservative to design the liner to withstand the unrestrained distortions of the medium. However, this approach may be unduly conservative for stiff liners, and the liner may become very difficult to design. In such cases, the ground/structure interaction is important and should be considered in the design.

Little attention has been devoted to deriving analytical solutions for ground/structure interaction problems for the case of waves propagating along the axis of the structure. This is due, in part, to the fact that several assumptions or approximations are needed to derive a solution for a simple ground/structure model. These assumptions restrict the application of the results to a limited class of problems. This ground/structure interaction problem has first been addressed in the design of the Trans-Bay Tube of the San Francisco Bay Area Rapid Transport (Parsons Brinckerhoff 1960) system and, later, by the Japan Society of Civil Engineers (1975, 1977).

The analytical procedure for estimating strains and stresses experienced by a structure that resists ground motion are based on: (a) the theory of wave propagation in an infinite, homogeneous, isotropic, elastic medium; and (b) the theory of an elastic beam on an elastic foundation. The beam theory is necessary to account for the effects of interaction between the ground and the structure. The details of this procedure and the assumptions made to arrive at a "closed-form solution" are discussed in detail in Appendix C. Its application in design is summarized below, under "Recommended Procedures for Preliminary Design of Underground Structures."

A main assumption in the above procedure is that the structure is supported by an elastic foundation characterized by a foundation modulus. The latter is defined as a spring constant per unit length of structure. Unfortunately, there is no universally agreed upon approach for the derivation of the foundation modulus; and different procedures may yield widely different answers. One approach, presented in Appendix C, is based on the two-dimensional, plane strain solution to the Kelvin's problem. The approach, in effect, neglects the width of the structure and, therefore, its transverse stiffness.

A more general approach would be to use a numerical solution to derive the foundation modulus. Numerical solutions require the use of a computer program, such as a large general-purpose finite element code; they are described below. Regardless of how the foundation modulus is obtained, a range of values, rather than a single value, should be used in parametric analyses to estimate bounds on the strains and stresses experienced by the structure and ground medium due to dynamic loading.

We believe that simple models for the ground/structure interaction, when used in conjunction with relatively simple structural design models for liners, are generally adequate for preliminary design of underground excavations with internal structures or supports that resist ground deformation. Of course, there will be many instances in which the structure is either too complex or too important to rely on such simple procedures alone. In these cases, one of the numerical methods discussed below should be used.

Numerical modeling of ground structure interaction

In recent years, numerical modeling techniques have seen a tremendous growth and have been found to be very useful as tools for analysis. As opposed to closed-form analytical solutions, which exist for a relatively small class of problems, numerical methods can be used for analysis and design of complex structures. A large number of publications have covered the different numerical methods used to analyse wave propagation and ground/structure interaction problems (Desai and Christian 1977). Herein, an overview of the different numerical methods available is presented, followed by a very brief summary of some popular computer programs used for the dynamic analysis of underground structures.

The numerical methods of analysis fall under one of the following categories: (a) finite difference method; (b) finite element method; (c) boundary integral equation method; and (d) method of characteristics. The usefulness, validity and application of each of these methods greatly depends on the type of problem under consideration.

The **finite difference method** was the main method of analysis before the development of finite element methods. The method involves a discretization of the governing equations of motion for the soil/structure system. The discretization is based on replacing the continuous derivatives in the governing equations by the ratio of changes in the variables over a small, but finite, increment. The differential equations are, thus, transformed into difference equations. The method of solution of these equations for transient analysis can be based on either an implicit scheme or an explicit scheme. The implicit scheme requires the solution of a set of simultaneous equations and large storage may be needed. Explicit schemes are relatively straightforward and may require less effort than implicit schemes. For certain types of problems, it is possible to obtain unconditionally stable implicit schemes. The choice of the best solution scheme depends on the particular application.

The finite difference method can be difficult to apply when nonhomogeneity and nonlinearities exist; however, this difficulty can be overcome using the so-called integrated finite difference techniques. Another situation common in wave propagation problems involves infinite media. Accordingly, there is a need to create appropriate boundary conditions that will simulate the physical behavior of the actual problem. The most popular approach is the use of viscous dashpots to eliminate boundary reflections.

In the **finite element method**, the continuum is discretized into an equivalent system of smaller continua, which are called finite elements. Each element is assigned constitutive or material properties and its equations of state are formulated. Subsequently the elements are assembled to obtain equations for the total structure. As in the case of the finite difference method, the solution scheme can be based on either an implicit or an explicit formulation. In either case, a finite difference approximation is used to represent the time dimension. The main advantage of the finite element method is that arbitrary boundaries and material inhomogeneity can be accommodated easily. As in the finite difference method, energy-absorbing boundaries are used to approximate the wave propagation in an infinite medium.

The **boundary integral equation method** involves numerical solution of a set of integral equations that connect the boundary, or surface, tractions to the boundary displacements. It is based on solution of integral, rather than differential, equations. It requires the discretization of only the surface of the body and the surface of the excavation into a number of segments or elements. The numerical solution is first obtained at the boundary segments; then the solution at different points within the medium is obtained from the solution at the boundary. In this method, the infinite medium can be handled very easily because the integral equation applies for a load applied on an infinite or semi-infinite medium. This method is most popular for the analysis of linear, static problems. Recently it has been applied to the solution of linear dynamic problems and to the analysis of traveling wave effects on the seismic response of surface structures (Werner et al. 1979). To date, it has not been widely

used to handle material non-linearities and nonhomogeneities.

The remaining approach is the **method of characteristics**. In this method, a set of partial differential equations is converted into a set of ordinary differential equations. The latter set often is solved by using the finite difference method.

Computer programs for dynamic analysis

Many computer programs based on the above analytical procedures are available. A few of the more popular, readily available codes that are well suited for investigating the problems of wave propagation and ground/structure interaction are described below.

SHAKE Code (Schnabel et al. 1972). This code can be used to analyse the free-field response. The soil medium comprises a system of horizontal viscoelastic layers of infinite horizontal extent, and an equivalent linear model is used to represent the strain dependence of the material properties of each soil layer. The medium can be subjected to input motion from vertically incident shear waves or compressional waves. A continuum solution to the one-dimensional wave equation is employed. The solution is carried out in the frequency domain and is then transformed back into the time domain through the use of Fast Fourier Transform techniques.

FLUSH Code (Lysmer et al. 1975). This code can be used to compute the two-dimensional response of a soil/structure system. Similar to the SHAKE code, the soil medium comprises a system of homogeneous viscoelastic soil layers of infinite horizontal extent; and an equivalent linear model is used to represent the strain-dependent shear moduli and damping ratios. The medium can be subjected only to vertically incident shear waves or compressional waves. The soil/structure system can be modeled using either a conventional plane strain model or a modified two-dimensional model that attempts to simulate three-dimensional wave propagation effects through the use of in-plane viscous dampers attached to each nodal point of the soil medium. The soil medium is bounded by a rigid base and by transmitting boundaries (viscous dashpots) along the sides. The solution technique is the same as that used for the SHAKE code.

ADINA Code (Adina Engineering 1981). This code is a general purpose finite element program for the two-dimensional and three-dimensional analysis, static and dynamic analysis of structural systems. Its library of elements includes structural as well as solid elements, and the library of constitutive models permits analysis of linear and nonlinear materials. The input motion can consist of horizontal and vertical motions from any arbitrary combinations of waves. The infinite medium is approximated by the use of transmitting boundaries (viscous dashpots). Several solution techniques are available. These include direct time integration method (with both explicit and implicit formulations), normal mode method for linear dynamic analysis, and determination of frequencies and mode shapes. Similar capabilities are offered by other general-purpose finite element codes such as SAPIV (Bathe et al. 1974) and ABAQUS (Hibbit et al. 1982).

HONDO Code (Key et al. 1978). This finite element program can be used to analyze two-dimensional wave propagation and soil/structure interaction problems. The medium is modeled with four-node quadrilateral element. Both linear and non-linear material behavior can be considered. The solution scheme is explicit, with a variable integration time step. In a recent version of the code, the medium can be bounded with energy-absorbing boundaries (viscous dashpots) in order to simulate an infinite medium. The code accepts only pressure loading. Similar capabilities are offered by other finite element codes, such as DYNA2D (Hallquist 1978), and finite difference codes, such as STEALTH (Hoffman 1981).

Recommended Procedures for Preliminary Design of Underground Structures

Despite the availability of relatively sophisticated methods of investigating the dynamic response of underground structures to seismic loading, design tools remain relatively simple. This section includes recommendations of simple procedures to facilitate identification of factors important to design, to define design loads, and to verify design adequacy. These, or similar procedures, should always be used as a starting point for any analyses of subsurface excavations and their ground support system, and underground structures.

Should the results of preliminary evaluation suggest that special precautions will be required to assure acceptable performance, then more rigorous analyses may be justified. However, care must be exercised to ensure that the refined methods will, indeed, lead to an improved solution. Often the uncertainty in the data defining the problem will be sufficient to deter more detailed analyses, and the improvement offered by detailed analyses may be illusory rather than real.

Design Against Fault Displacement

It is impractical to attempt to design a tunnel to withstand a potential offset at an active fault. Instead, features that mitigate the effect of the offset and facilitate post-earthquake repairs should be incorporated in the design. These features typically consist of either (1) excavation of an oversize section through the fault zone and use of a flexible support system; or (2) incorporation of a flexible coupling, if the tunnel is lined. The former approach was used where the San Francisco Bay Area Rapid Transit (SFBART) crosses the Hayward fault in the Berkeley Hills; a slightly enlarged section in the vicinity of the fault was lined with closely spaced steel rib sections (Kuesel 1968). The latter approach is more commonly used for submerged tunnels or conduits, since in these cases it is necessary to ensure that the section remains watertight.

The design of flexible couplings, or joints, has received considerable attention because they are also required at interfaces between different geologic media and between sections of an underground structure that will respond differently to seismic loading. For example, the ASCE Working Group for Seismic Response of Buried Pipes and Structural Components provide details of an interface between buildings and buried pipes (ASCE 1983); Douglas and Warshaw (1971) describe a seismic joint used at the transition between the SFBART tube and an offshore ventilation structure; and Hradilek (1977) offers recommendations for the design of reinforced concrete conduits crossing a known active fault zone. In every case the design objective is to achieve the necessary flexibility in the liner, or conduit, to permit the relative motion without significant damage. How this objective is achieved will be site specific and project specific.

Design of Portals and Very Shallow Tunnels

It was noted above that tunnel portals appear to be particularly susceptible to damage. This may be attributed to the occurrence of superficial failures that may be entirely unrelated to the tunnel, or may result from transition problems such as described above. The site investigation required to determine the potential for superficial failures is beyond the scope of this study. However, it is appropriate to note that the principal failure modes of concern are slope instability, soil liquefaction, and differential settlement. Particular precautions should be taken if a portal structure also acts as a soil retaining wall.

Design to withstand relative motion has been discussed above. As noted, the primary objective is to increase the flexibility so that differential motion can be survived without significant damage. For tunnels in soil or rock, such flexibility is best provided by closely spaced steel sets, or ribs. Static design procedures for this type of support are relatively well-established.

Special design considerations for flexible support in a dynamic environment are discussed below.

Design Against Ground Shaking

Discussion in this section is restricted to consideration of simplified models that may be used to estimate the stresses and strains that an underground excavation may be subjected to as a result of ground shaking during an earthquake, and the resulting additional dynamic loads that will be applied to a support system. Types of excavation for which these models are appropriate include lined and unlined tunnels in soil and rock, subaqueous tunnels, and cut-and-cover construction. The distinction between the several types is drawn not upon the basis of the function that the excavation serves but upon: (a) the nature of the geologic medium; (b) the extent to which any support system may resist the ground motion in the medium; and (c) the method of construction.

Before proceeding it is worthwhile to clarify the terminology that will be used, and to elaborate on the subject of ground/structure interaction. From an analytical standpoint, the simplest case to consider is that of a compressional wave propagating parallel to the axis of a subsurface excavation. That case is illustrated in Fig. 7, in which the wave is shown as introducing longitudinal compression and tension. For practical purposes, interaction between the wave and the excavation can be ignored, although the changes in axial stress will cause some closure or enlargement of the excavation as the rock or soil responds to the applied loads.

The case of an underground structure subjected to an axially propagating wave is slightly more complex since there will be some interaction between the structure and the medium. However, the interaction is likely to be relatively unimportant because the induced stresses normal to the axis of the tunnel will be less than if the wave were propagating normal to the tunnel axis. Also, the deformation mode would be one of hydrostatic compression or tension.

For the case of a wave propagating normal to the tunnel axis, the stress induces a deformation of the cross-section, such as that illustrated in Fig. 8. As discussed heretofore, the type of asymmetric deformation of the cross-section illustrated in that figure will be observed only if the wavelength is short relative to the tunnel diameter. In most cases of interest, the wavelength will be relatively long and the deformation will be approximately pseudostatic. Expressed simply, that means that the tunnel is not subjected to any severe stress gradients, and, therefore, the deformation will appear to be symmetrical about the center plane of the section. However, the deformed shape of the tunnel still will be approximately elliptical because the free-field stresses in the direction of propagation and normal to the direction of propagation will be unequal.

In the more general case, the wave may induce curvature of the structure in the manner illustrated in Fig. 9. This phenomenon will induce alternate regions of compression and tension along the tunnel. In a subsurface excavation, or one with a very flexible liner, the rock or soil mass will experience tension and compression on opposite sides; in the region of positive curvature, the tension is on the side marked "top", and compression is on the side marked "bottom". In contrast, a stiff lining would experience com-

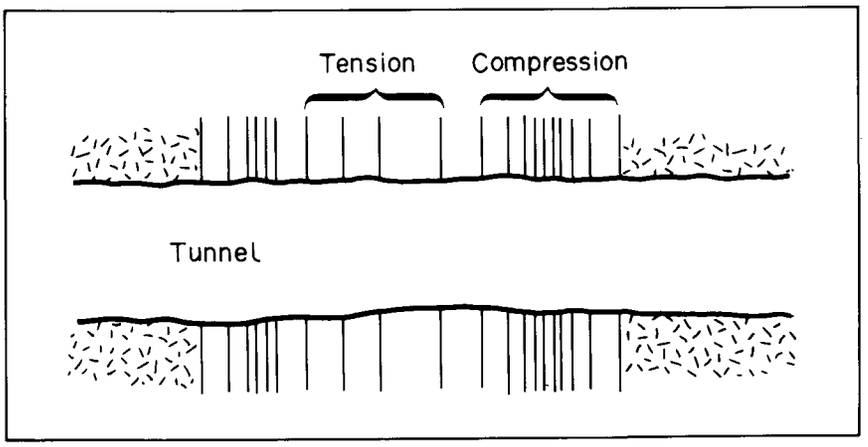

Figure 7. Axial deformation along a subsurface excavation (from Owen and Scholl 1981).

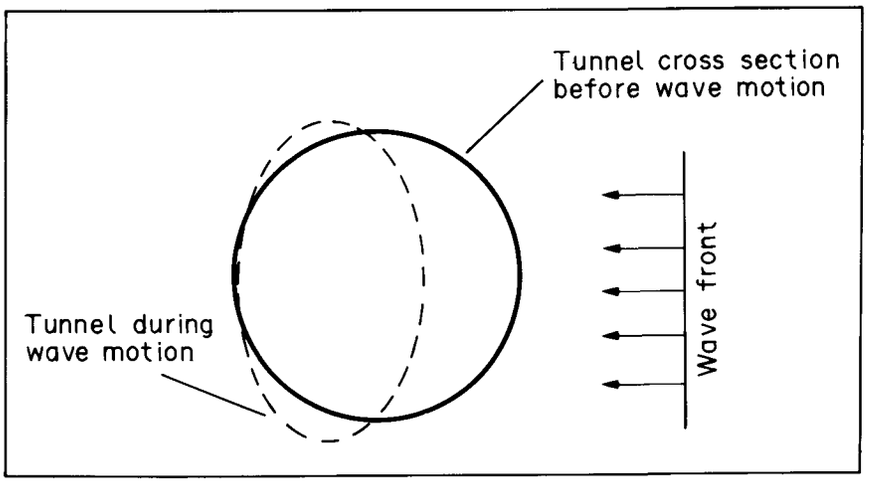

Figure 8. Hoop deformation of cross-section (from Owen and Scholl 1981).

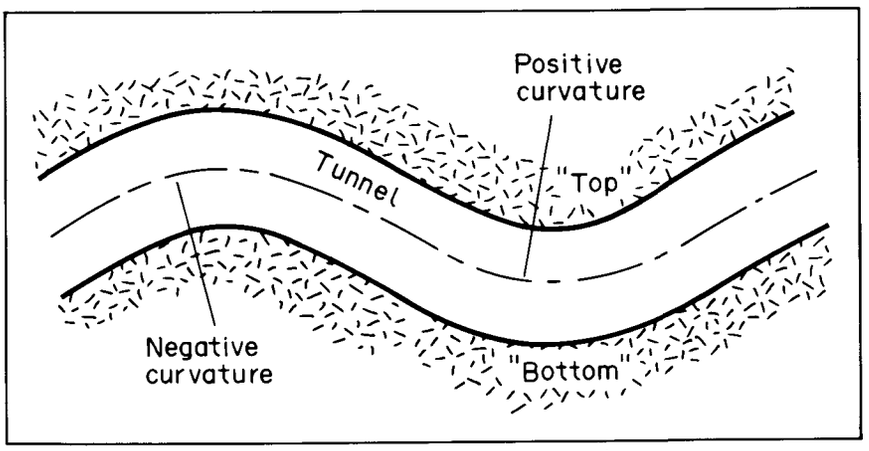

Figure 9. Curvature deformation along a tunnel (from Owen and Scholl 1981).

pression in the top and tension in the bottom, because the stiff liner would resist the deformation of the medium. This idea of relative stiffness and the concept of interaction of the liner, or ground support system, and the medium are important to the discussion that follows.

Structures that conform to ground motion

In this case any liner or internal structure is considered to offer little or no resistance to ground motion. The case is pertinent to most tunnels in rock and many soils, since the liner stiffness is low in comparison to that of the medium. A full description of the derivation of the equations included in this section and a discussion of the assumptions made in order to derive these equations are included in Appendix B. The following is a summary of the theoretical basis and the recommended design procedure.

The analytical procedure for estimating strains and stresses experienced by structures that conform to the ground motion during seismic excitation is based on the theory of wave propagation in homogeneous, isotropic, elastic media (Newmark 1967). Starting from the equation describing particle motion resulting from propagation of a plane wave in the x-direction, it can be shown that the axial strain $(\partial u/\partial x)$ and curvature $(\partial^2 u/\partial x^2)$ in the direction of propagation are, respectively:

$$\frac{\partial u}{\partial x} = -\frac{1}{c}\frac{\partial u}{\partial t} \quad ; \quad \frac{\partial^2 u}{\partial x^2} = \frac{1}{c^2}\frac{\partial^2 u}{\partial t^2} \qquad (16)$$

in which $(\partial u/\partial t)$ and $(\partial^2 u/\partial t^2)$ are the particle velocity and acceleration; t, the time; and c, the apparent wave propagation velocity.

The strains and curvatures experienced in the free field in response to different wave types can be evaluated from Equation (16). For example, in the case of a P-wave, for which the particle motion is in the direction of wave propagation, the axial or longitudinal strain (ϵ_l) and its peak value (ϵ_{lm}) are given by:

$$\epsilon_l = \frac{\partial u_l}{\partial l} \quad ; \quad \epsilon_{lm} = \pm\frac{V_p}{c_p} \qquad (17)$$

in which c_p is the P-wave velocity and V_p, the peak particle velocity. The corresponding strain normal to the direction of propagation and the shear strain are both zero.

Similarly, the maximum shear strain (and the curvature $(1/\rho_m)$ due to an S-wave) are given by:

$$\gamma_m = \frac{V_s}{c_s} \quad ; \quad \frac{1}{\rho_m} = \frac{a_s}{c_s^2} \qquad (18)$$

in which c_s is the S-wave velocity; V_s, the maximum particle velocity; and a_s, the maximum particle acceleration. In this case, there are no axial or normal strains.

Equations (17) and (18) describe the strains and curvature in the direction of propagation of P- or S-waves. In the more general case, the P- or S-wave propagates at an angle ϕ with respect to the axis of some excavation or structure within the medium. The corresponding strains and curvatures, expressed as a function of the angle of incidence, are summarized in Table 1. Because the angle of incidence is generally not known, the most critical angle of incidence and the maximum values of strain and curvature are also tabulated. Similar data are provided for Rayleigh waves. Estimation of the peak ground motion characteristics (velocity and acceleration) is discussed in Appendix A.

After the strains have been evaluated, the free-field stresses can be estimated by assuming that the medium can be treated as a linear elastic material. On that basis, the maximum stresses resulting from P- and S-waves listed in Table 2 were derived. These are, of course, the free-field stresses that would be used as boundary conditions if simple continuum models are to be used for design of lined or unlined tunnels. If, instead, the tunnel structure is treated as a

Table 1. Strain and curvature due to body and surface waves.

Wave Type		Longitudinal strain	Normal strain	Shear strain	Curvature
P-Wave		$\epsilon_l = \frac{V_p}{c_p}\cos^2\phi$	$\epsilon_n = \frac{V_p}{c_p}\sin^2\phi$	$\gamma = \frac{V_p}{c_p}\sin\phi\cos\phi$	$\frac{1}{\rho} = \frac{a_p}{c_p^2}\sin\phi\cos^2\phi$
		$\epsilon_{lm} = \frac{V_p}{c_p}$ for $\phi = 0°$	$\epsilon_{nm} = \frac{V_p}{c_p}$ for $\phi = 90°$	$\gamma_m = \frac{V_p}{2c_p}$ for $\phi = 45°$	$\frac{1}{\rho_m} = 0.385\frac{a_p}{c_p^2}$ for $\phi = 35°16'$
S-Wave		$\epsilon_l = \frac{V_s}{c_s}\sin\phi\cos\phi$	$\epsilon_n = \frac{V_s}{c_s}\sin\phi\cos\phi$	$\gamma = \frac{V_s}{c_s}\cos^2\phi$	$K = \frac{a_s}{c_s^2}\cos^3\phi$
		$\epsilon_{lm} = \frac{V_s}{2c_s}$ for $\phi = 45°$	$\epsilon_{nm} = \frac{V_s}{2c_s}$ for $\phi = 45°$	$\gamma_m = \frac{V_s}{c_s}$ for $\phi = 0°$	$K_m = \frac{a_s}{c_s^2}$ for $\phi = 0°$
Rayleigh wave	Compressional component	$\epsilon_l = \frac{V_{RP}}{c_R}\cos^2\phi$	$\epsilon_n = \frac{V_{RP}}{c_R}\sin^2\phi$	$\gamma = \frac{V_{RP}}{c_R}\sin\phi\cos\phi$	$K = \frac{a_{RP}}{c_R^2}\sin\phi\cos^2\phi$
		$\epsilon_{lm} = \frac{V_{RP}}{c_R}$ for $\phi = 0°$	$\epsilon_{nm} = \frac{V_{RP}}{c_R}$ for $\phi = 90°$	$\gamma_m = \frac{V_{RP}}{2c_R}$ for $\phi = 45°$	$K_m = 0.385\frac{a_{RP}}{c_R^2}$ for $\phi = 35°16'$
	Shear component		$\epsilon_n = \frac{V_{RS}}{c_R}\sin\phi$	$\gamma = \frac{V_{RS}}{c_R}\cos\phi$	$K = \frac{a_{RS}}{c_R^2}\cos^2\phi$
			$\epsilon_{nm} = \frac{V_{RS}}{c_R}$ for $\phi = 90°$	$\gamma_m = \frac{V_{RS}}{c_R}$ for $\phi = 0°$	$K_m = \frac{a_{RS}}{c_R^2}$ for $\phi = 0°$

Table 2. Maximum stresses resulting from body waves.

	Maximum normal stress	Maximum shear stress
P-wave	$\frac{(1-\nu)E}{(1+\nu)(1-2\nu)} \frac{V_p}{c_p}$	$\frac{G}{2} \frac{V_p}{c_p}$
S-wave	$\frac{E}{(1+\nu)(1-2\nu)} \frac{V_s}{2\ c_s}$	$\frac{G}{c_s} \frac{V_s}{}$
	$\phi = 45°$	$\phi = 0$

simple beam, then the design strains and curvatures are given directly by Table 1. The design stresses then can be easily calculated by using the equations of the beam theory.

Box structures in rock and stiff soil are subject to racking deformations due to shear distortions in the medium. The amount of racking imposed on the structure is estimated on the basis of the assumed soil deformations. The analytical solution of the one-dimensional wave propagation problem for SH-waves, described above, or a computer program such as SHAKE can be used to estimate the free-field shear deformations vs depth at a given site. An example of the soil deformation with depth is shown in Fig. 10a. The amount of racking imposed on the structure can be taken as equal to the difference between the soil deformations at the top and that at the bottom of the structure, such as points A and B in Fig. 10b. The structure needs to be designed to accommodate that amount of deformation—providing, of course, that toleration of such deformation does not jeopardize safety or functional requirements.

The above approach to design of underground structures may lead to very conservative design requirements if the structure is very stiff relative to the medium. This is the case for structures with shear walls, for example. In these circumstances a numerical analysis of the soil/structure interaction becomes necessary. In general, a relatively simple two-dimensional parametric analysis of a structure such as the one illustrated in Fig. 10b is all that is needed. A general purpose computer program for structural analysis, such as ADINA code, normally would be appropriate. The results of such an exercise would be used to determine the relative properties of soil and structure for which the interaction becomes important; and to refine the estimate of racking deformation imposed on the structure. The latter should be smaller than the racking estimated on the basis of the free-field deformations.

Structures that resist ground motion

In this case, the liner or internal structure is considered to resist the ground motion; ground/structure interaction is important because the structure is stiff relative to the surrounding medium. Although the case is usually pertinent only to structures in soft soil, it is always advisable to check the relative stiffness of the ground and any lining or internal structure. The results presented herein comprise further development of the work of several investigators, including Kuesel (1969) and Kuribayashi et al. (1975, 1977). Again, a summary of theoretical development and the recommended design procedure are presented below. Additional information on the theoretical background is provided in Appendix C.

The analytical procedure for estimating strains and stresses experienced by structures that resist the ground motion during seismic excitation is based on the theory of wave propagation in an infinite, homogeneous, isotropic, elastic medium, together with the theory for an elastic beam on an elastic foundation. The beam theory is necessary to account for the effects of interaction between the soil and the tunnel structure. In the interest of brevity, only the effects of transverse shear waves are discussed herein. However, the same approach can be used to evaluate the effects of vertical shear waves and compressional waves.

A tunnel structure subjected to an incident sinusoidal shear wave with a wavelength L and amplitude A, as shown in Fig. 11, will experience transverse and axial displacements:

$$u_y = \cos\phi \sin\left(\frac{2\pi x}{L/\cos\phi}\right)A \ ; \qquad u_x = \sin\phi \sin\left(\frac{2\pi x}{L/\cos\phi}\right)A \ . \tag{19}$$

Assuming the structure behaves like a beam, the curvature due to transverse displacement is given by:

$$\frac{1}{\rho} = \frac{\partial^2 u_y}{\partial x^2} = -\left(\frac{2\pi}{L}\right)^2 \cos^3\varphi \sin\left(\frac{2\pi x}{L/\cos\phi}\right)A \ . \tag{20}$$

The resulting forces and bending moments experienced by the structure are identified in Fig. 12 and can be easily calculated if there is no ground/structure interaction. However, if the structure is stiffer than the surrounding medium it will distort less than the free ground deformations, and there will be interaction between the tunnel structure and surrounding medium. This interaction can be considered simply if it is assumed that the tunnel structure behaves as an elastic beam supported on elastic foundation. However, this approach involves estimating the foundation modulus.

To arrive at an estimate for the foundation modulus, the two-dimensional, plane-strain solution to the Kelvin's problem was used. The equation defining the vertical displacement due to a point load was

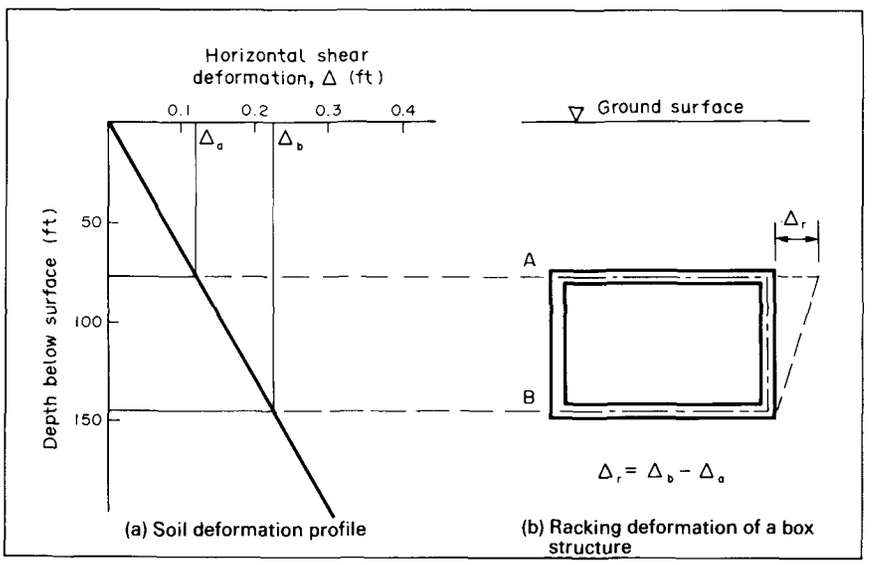

Figure 10. Typical soil deformation profile and racking imposed on an underground structure during an earthquake.

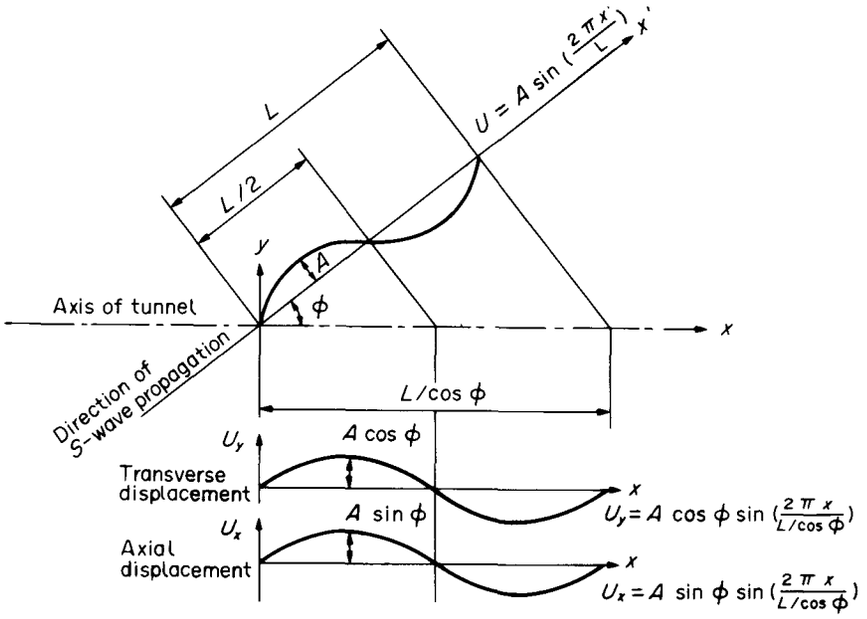

Figure 11. Displacements due to shear-wave propagation.

integrated numerically to study the effect of a displacement that is sinusoidally varying. From the results of those calculations, and the general form of Kelvin's solution, the foundation modulus for the transverse deformations was deduced to be:

$$K_h = \frac{2\pi C}{L} \; ; \quad C = \frac{4\,(1-\nu)}{(3-4\nu)\,(1+\nu)} E\,d \qquad (21)$$

where d represents the width of the tunnel, and E and ν are medium properties. This modulus is consistent with that derived by Biot (1965) for the case where the medium is compressible.

The expressions for the forces applied on the structure can be obtained from the solution of the governing equations given above. These expressions need to be maximized with respect to the wavelength, L, and the angle of incidence, ϕ (see Appendix C). The results are summarized in Table 3 for the case of transverse-horizontal and transverse-vertical shear waves.

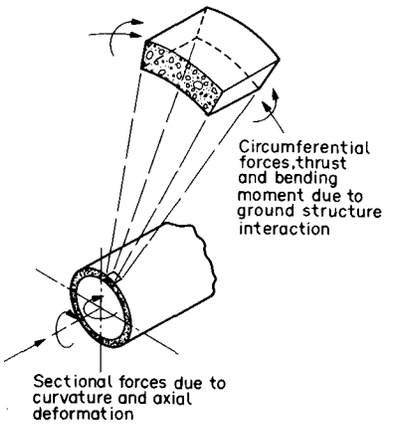

Figure 12. Identification of design parameters for a tunnel section (modified from Owen and Scholl 1981).

Ground motion displacement spectrum

In order to calculate the design forces using the equations listed in Table 3, the ground displacement amplitude (A) must be estimated. One approach would be to estimate the natural period of the ground that is used to enter a ground motion spectrum and pick the displacement amplitude. The following paragraphs summarize methods for deriving a ground motion spectrum, and for estimating the natural period of the ground.

The procedure used to select a design spectrum for surface structures is discussed in Appendix A; it is based primarily on strong motion data from surface records, considered in conjunction with specified design levels of structural resistance. However, because ample strong motion data generally are not available at the depths of concern for design of underground structures, the development of a ground motion spectrum for use in design of these structures requires alternative approaches that incorporate depth-dependent attenuation effects. One such approach uses site response analysis techniques to compute free-field motions at any desired depth, considering soil properties of the actual site profile under consideration. One-dimensional analysis procedures are most widely used for this purpose, although it

Table 3. Maximum forces resulting from shear waves.

I. Transverse-horizontal waves

Bending moment = $\frac{1}{3}(4\,EIC^2)^{1/3} A$

Shear force = $C\,A$

Axial force = $C\,A$

Pressure = $\frac{4}{5}\left(\frac{4C^4}{E\,I}\right)^{1/3} A$

where $C = \frac{4(1-\nu)}{(3-4\nu)(1+\nu)} Ed$

and A corresponds to the amplitude of the horizontal motion

II. Transverse-vertical waves

Bending moment = $\frac{1}{3}(4\,EIB^2)^{1/3} A$

Shear force = $B\,A$

Axial force = $C\,A$

Pressure = $\frac{4}{5}\left(\frac{4B^4}{E\,I}\right)^{1/3} A$

where $B = \frac{Ed}{2(1-\nu)(1+\nu)}$

and A corresponds to the amplitude of the vertical motion

E = modulus of elasticity of concrete;
I = moment of inertia of tunnel cross-section;
d = width of tunnel;
E = modulus of elasticity of soil medium;
ν = Poisson's ratio of soil medium.

should be noted that such procedures ignore effects from all but vertically propagating body waves.

Two types of site response analyses can be used to compute free-field motions at depth. One type uses a deconvolution procedure, consisting of definition of input motions at the ground surface and use of the one-dimensional wave equation to compute the corresponding subsurface motions. However, because results from this procedure can be quite sensitive to uncertainties in definition of surface input motions and/or subsurface soil properties, care must be taken both in its application and during interpretation of its results (Schnabel et al. 1972).

In the second type of site response analysis, surface motions are applied at the subsurface soil/rock interface and the motions at the ground surface are calculated. The calculated surface motions are then scaled so that some measure of their strength, e.g. their spectrum intensity, or the area under the response spectrum over the frequency range of interest, is identical to that of certain designated surface motions. The scale factor then can be applied to the calculated motions at the required depths. By repeating this calculation for a range of soil properties and input ground motion, a plot of the ground motion displacement amplitude as a function of the natural period of the ground can be derived. This plot of the ground displacement amplitude at the depth of concern is referred to as the ground motion spectrum.

The final stage in determining the displacement amplitude of ground motion is to estimate the natural period for the site and then use that to enter the ground motion spectrum. The natural period can be calculated easily if the earthquake ground motion is attributed primarily to shear waves and it can be assumed that the medium consists of a uniform soil layer overlaying a hard layer. In these circumstances the ground deformation may be approximated by an arc of a sine curve, as shown in Fig. 13. The dynamic response of this medium is analogous to that of a shear beam subjected to a base motion. In this case, the natural period of the ground is given by

$$T = \frac{4H}{c_s} \tag{22}$$

where H represents the thickness of the soil layer and c_s, the shear wave velocity. Thus, the period is equal to the time it takes a shear wave to travel four times the thickness of the soil; or, in other words, to repeat itself. The case of a medium with several horizontal soil layers is covered by Idriss and Seed (1968).

Cut-and-cover construction

Cut-and-cover construction is treated as an independent topic merely because it involves substantially different construction practice than other forms of underground excavations. Typically, a backfill is placed between the medium and the underground excavation, and that backfill may consist of relatively poorly compacted material. Despite these differences, the methods of design are identical. It is recommended that an approach similar to that described in the previous sections be used.

The major difference is that under horizontal shear waves (SH-waves), the foundation modulus or spring constants in the soil/structure interaction model should reflect the properties of the interface material between structure and soil. Since in this model the spring constant is based on the assumption of a uniform rather than layered medium, two cases may be considered in order to bound the problem. In one case, the spring constant is based on the properties of the backfill; and, in the other, it is based on the properties of the medium. It is believed that such an approach will prove to be conservative and realistic.

Under vertical shear waves (SV-waves), the ground support is placed in direct contact with the medium. As a result, the same procedure outlined in the previous sections applies in this case.

Acknowledgements—This report is based on research supported by the National Science Foundation (NSF), under Grant No. CEE-8310631. In that regard, the authors particularly acknowledge the interest and active support of Drs William Hakala and K. T. Thirumalai of the NSF. Without such support, the undertaking of this research would not have been practical.

The authors also gratefully acknowledge the effort of the following individuals who reviewed various drafts of the report and provided very necessary constructive criticism: Dr M. S. Agbabian (Department of Civil Engineering, University of Southern California); Dr C. H. Dowding (Department of Civil Engineering, Northwestern University); Dr W. J. Hall (Department of Civil Engineering, University of Illinois); Dr F. E. Heuze (Lawrence Livermore National Laboratory); Dr D. A. Howells (Independent consultant, U.K.); Dr J. E. Monsees (Parsons, Brinckerhoff, Quade & Douglas, Inc.); and Dr G. N. Owen (URS/Blume Engineers).

Particular acknowledgement is due Mr S. D. Werner, of Agbabian Associates, who reviewed drafts of the report and contributed directly in preparation of the section entitled "Seismic Activity" and Appendix A. Last, but by no means least, we acknowledge the assistance and patience of Agbabian Associates Publications Staff: Judith Rubottom, Pat LaPonza, Jack Peters, and Evelyn Harding.

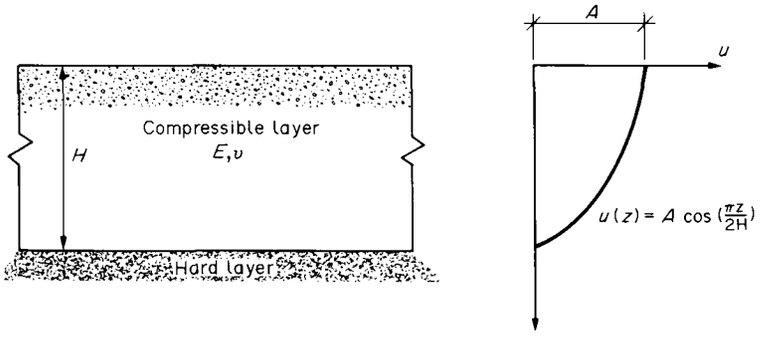

Figure 13. Soil properties.

Bibliography

Achenbach, J. D. 1975. *Wave Propagation in Elastic Solids*. New York: North-Holland/American Elsevier.

Adina Engineering. 1981. ADINA users manual. Report AE81-1. Watertown, MA: ADINA Eng.

Agbabian Associates (AA). 1985. Baseline dynamic analyses in support of supplemental seismic design criteria—Metro rail project. Report No. R-8513-5884. El Segundo, CA: AA.

Algermissen, S. T. and Perkins, D. 1976. A probabilistic estimate of maximum acceleration in rock in the contiguous United States. Open File Report 76-416. Arlington, VA: U.S. Geol. Survey.

American Society of Civil Engineers. 1983. Seismic response of buried pipes and structural components. Report by Seismic Analysis Committee of ASCE Nuclear Structures and Materials Committee.

Applied Technology Council (ATC). 1978. Tentative provisions for the development of seismic regulations for buildings. Report No. ATC 3-06, 514 pp. Washington, DC: USGPO.

Ariman, T. 1977. A review of the earthquake response and aseismic design of underground piping systems. *Proc. Lifeline Earthquake Eng. Specialty Conf., ASCE*, pp. 282-292.

Barton, N. 1981. Importance of joint parameters on deformations observed in dynamically loaded models of large excavations. *Proc. Workshop Seismic Performance of Underground Struc.*, DE-1623, pp. 243-248. Aiken, SC: du Pont de Nemours, Savannah River Laboratory.

Bathe, K. J. et al. 1974. SAP IV, A structural

analysis program for static and dynamic response of linear systems. Report No. EERC 73-11. Berkeley: Univ. of Cal.

Berg, G. V. 1982. *Seismic Design and Procedures*. Berkeley, CA: Earthquake Eng. Research Institute.

Biot, M. S. 1965. *Mechanics of Incremental Deformations*. New York: Wiley.

Blume, J. A. 1972. Surface and subsurface ground motion. *Proc. Eng. Foundation Conf. on Earthquake Protection of Underground Utility Structure*, Asilomar, CA.

Bolt, B. A. 1978. *Earthquakes, A Primer*. San Francisco: W. H. Freeman.

Boore, D. M. and Joyner, W. B. 1982. The empirical prediction of ground motion. *Bull. seism. Soc. Am.* **72B**(6): S43-S60.

Brown, I. R., Brekke, T. L. and Korbin, G. E. 1981. Behavior of the Bay Area Rapid Transit tunnels through the Hayward Fault. U.S. Dept. of Transportation Report No. UMTA-CA-06-0130-81-1.

Campbell, K. W. 1981. Near-source attenuation of peak horizontal acceleration. *Bull seism. Soc. Am.* **71**(6): 2039-2070.

Coal Mines Planning and Design Institute (CMPD). 1982. Damage to structures and installations in the underground excavations of the Kailuan colliery during the Tangshan earthquake. *Earthquake Engng Engng Vibration* **2**:1. Ministry of Coal Industry, China.

Cooke, J. B. 1971. Earthquake risk—Savannah bedrock storage project. Consulting Report to the Savannah River Project, U.S. Army Corps of Engineers Waterways Experiment Station, Vicksburg, MS.

Cording, E. J. 1971. Rock engineering for underground caverns. *Symp. on Underground Rock Chambers, Phoenix*, pp. 567-600.

Crouch, S. L. and Starfield, A. M. 1983. *Boundary Element Methods in Solid Mechanics*. Winchester, MA: Allen & Unwin.

Cundall, P. A. 1971a. The measurement and analysis of accelerations in rock slopes. Ph.D Thesis. Imperial College, London University, London.

Cundall, P. A. 1971b. A computer model for simulating progressive, large scale movements in blocky rock systems. *Symp. Int. Rock Mech. Soc., Nancy, France*.

Cundall, P. and Hart, R. 1983. Development of generalized 2-D and 3-D distinct element programs for modeling jointed rock. Final Tech. Report. Prepared by Itasca Consult. Eng. for U.S. Army Waterways Exp. Sta., Vicksburgh, MS.

Desai, C. S. and Christian, J. T. 1977. *Numerical Methods in Geotechnical Engineering*. New York: McGraw-Hill.

Donovan, N. C. 1982. Strong motion attenuation equations—A critique, *Proc. 3rd Int. Earthquake Microzonation Conf., Seattle*, June-July, Vol. 1, pp. 377-388.

Douglas, W. S. and Warshaw, R. 1971. Design of seismic joint for San Francisco Bay Tunnel. *J. struct. Div. Am. Soc. civ. Engrs.* **97**(ST4): 1129-1141.

Dowding, C. H. 1977. Seismic stability of underground openings. *Proc. Rockstore Conf., Stockholm*.

Dowding, C. H. and Rozen, A. 1978. Damage to rock tunnels from earthquake shaking. *J. geotech. Engng Div. Am. Soc. Civ. Engrs* **104** (GT2): 175-191.

Dowding, C. H., Ho, C. and Belytschko, T. B. 1983. Earthquake response of caverns in jointed rock: effects of frequency and jointing. *Seismic Design of Embankments and Caverns*. New York: ASCE.

Duddeck, H. and Erdman, J. 1982. Structural design models for tunnels. *Tunneling '82*, pp. 83-91. London: The Institute of Mining and Metallurgy.

Einstein, H. H. and Schwartz, C. W. 1979. Simplified analysis for tunnel supports. *J. geotech. Engng Div. Am. Soc. Civ. Engrs* **105**(GT4).

Emergy, J. J. and Joshi, V. H. 1980. Seismic response of underground openings. *Proc. 13th Canadian Rock Mechanics Symp., Toronto*, pp. 177-180.

Fung, Y. C. 1965. *Foundations of Solid Mechanics*. Englewood Cliffs, N.J.: Prentice-Hall.

Garnet, H. and Crouzet-Pascal, J. 1966. Transient response of a circular cylinder of arbitrary thickness, in an elastic medium, to a plane dilatational wave. *J. appl. Mech.* **33**: 521-531.

Gay, N. C., ed. 1980. Strong ground motion of mine tremors: some implications for near-source ground parameters. Chamber of Mines of South Africa, Research Report No. 32/80.

Glass, C. E. 1976. Seismic considerations in siting large underground openings in rock. Ph.D. dissertation, Univ. of California, Berkeley.

Goodman, R. E. and Shi, G. H. 1985. *Block Theory and Its Application in Rock Engineering*. Englewood Cliffs, N.J.: Prentice-Hall.

Goodman, R. E. and St John, C. M. 1977. Finite element analysis for discontinuous rocks. *Numerical Methods in Geotech. Eng.*, pp. 148-175. New York: McGraw-Hill.

Goodman, R. E., Shi, G. H. and Boyle, W. 1982. Calculation of support for hard, jointed rock using the keyblock principle. *23rd Symp. on Rock Mech., Univ. of Cal., Berkeley*, pp. 883-898.

Hallquist, J. D. 1978. DYNA2D—An explicit finite element and finite difference code for axisymmetric and plane strain calculations (Users Guide). Report No. UCRL-52429. Univ. of Calif.: Lawrence Livermore Natn. Lab.

Hamada, M., Akimoto, T. and Izumi, H. 1977. Dynamic stress of a submerged tunnel during earthquakes. *Proc. 6th World Conf. on Earthquake Eng., New Delhi, India*.

Hendron, A. J., Jr and Fernandez, G. 1983. Dynamic and static design considerations for underground chambers. *Seismic Design of Embankments and Caverns*, pp. 157-197. New York: ASCE.

Hibbitt, Karlsson and Sorensen Inc. 1982. *ABAQUS User's Manual*. Providence, RI: Hibbitt Karlsson and Sorenson, Inc.

Hoek, E. and Brown, E. T. 1981. *Underground Excavations in Rock*. London: The Institute of Mining and Metallurgy.

Hoffman, R. 1981. STEALTH—A lagrangian explicit finite difference code for solids, structural, and thermohydraulic analysis, introduction and guide. EPRI NP-2080-CCM-SY. Palo Alto, CA: Electric Power Research Inst.

Housner, G. W. 1959. Behavior of structures during earthquakes. *Proc. Engng mech. Div. Am. Soc. Civ. Engrs* **85**(EM4): 109-129.

Housner, G. W. and Jennings, P. C. 1982. Earthquake design criteria. EERI Monograph Series, Berkley, CA.

Hradilek, P. J. 1977. Behavior of underground box conduit in the San Fernando earthquake. *The Current State of Knowledge of Lifeline Earthquake Engineering*, pp. 308-319. New York: ASCE.

Idriss, I. M. and Seed, H. B. 1968. Seismic response of horizontal soil layers. *J. Soil Mech. Found. Div. Am. Soc. Civ. Engrs* **94**(SM4): 1003-1031.

Iida, K. 1965. Earthquake magnitude, earthquake fault, and source dimensions. *Nagaya Univ. J. Earth Sci.* **13**(2): 115-132.

Japan Society of Civil Engineers. 1975. *Specifications for Earthquake Resistant Design of Submerged Tunnels*. Tokyo.

Japan Society of Civil Engineers. 1977. *Earthquake Resistance Design Features of Submerged Tunnels in Japan*. Tokyo.

Johnson, J. N. and Schmitz, D. R. 1976. Incipient fault motion due to a spherical explosion. DNA 39481.

Joyner, W. B. and Boore, D. M. 1981. Peak horizontal acceleration and velocity from strong-motion records including records from 1979 Imperial Valley, California, earthquake. *Bull. seism. Soc. Am.* **71**(6): 2011-2038.

Joyner, W. B., Warrick, R. E. and Oliver, A. A. 1976. Analysis of seismograms from a downhole array in sediments near San Francisco Bay. *Bull. seism. Soc. Am.* **66**(3): 937-958.

Kanai, K. et al. 1966. Comparative studies of earthquake motions on the ground and underground II. *Bull. Earthq. Res. Inst.* **44**: 609-643.

Kanamori, H. and Anderson, D. L. 1975. Theoretical basis of some empirical relations in seismology. *Bull. seism. Soc. Am.* **65**(5): 1073-1095.

Key, S. W. et al. 1978. HONDO II—A finite element computer program for the large deformation dynamic response of axisymmetric solids. Sandia Natn. Lab.

Kuesel, T. R. 1968. Structural design of the Bay Area Rapid Transit System. *Civil Engng Am. Soc. Civ. Engrs* 46-50. New York.

Kuesel, T. R. 1969. Earthquake design criteria for subways. *J. struct. Div. Am. Soc. Civ. Engrs* **95**(ST6): 1213-1231.

Kuribayashi, E. and Kawashima, K. 1976. Earthquake resistant design of submerged tunnels and an example of its application. Tech. Memorandum No. 1169, Public Works Research Institute, Tsukuba, Japan.

Kuribayashi, E., Iwasaki, T. and Kawashima, K. 1975. Dynamic behavior of a subsurface tubular structure. *Proc. 5th European Conf. on Earthquake Engng, Istanbul*.

Kuribayashi, E., Iwasaki, T. and Kawashima, K. 1977. Earthquake resistance of subsurface tubular structure. *Proc. 6th World Conf. on Earthquake Engng, New Delhi, India*, Vol. 5.

Labreche, D. A. 1983. Damage mechanisms in tunnels subjected to explosive loads. *Seismic Design of Embankments and Caverns*, pp. 128-141. New York: ASCE.

Langefors, U. and Kihlstrom, B. 1963. *The Modern Technique of Rock Blasting*. New York: John Wiley and Stockholm, Sweden: Almquist & Wiksell.

Lysmer, J. et al. 1975. FLUSH—A computer program for approximate 3-D analysis of soil-structure interaction problems. Report No. EERC 75-30. Berkeley: Univ. of Calif.

McGarr, A. 1983. Estimated ground motion for small near-by earthquakes. *Seismic Design of Embankment and Caverns*, pp. 113-127. New York: ASCE.

McGuire, R. K. 1978. Seismic ground motion parameter relations. *J. geotech. Engng Div.* **104**(GT4): 481–490.
Marine, I. W., ed. 1981. *Proc. Workshop on Seismic Performance of Underground Facilities, Augusta, GA.* Springfield, VA: NTIS.
Mark, R. K. and Bonilla, M. G. 1977. Regression analysis of earthquake magnitude and surface fault length using the 1970 data of Bonilla and Buchanan. Open-File Report 77-614. Menlo Park, CA: U.S. Geological Survey.
Mow, C. C. and Pao, Y. H. 1971. The diffraction of elastic waves and dynamic stress concentrations. R-482-R. Santa Monica, CA: The Rand Corp.
Newmark, N. M. 1967. Problems in wave propagation in soil and rock. *Proc. Int. Symp. Wave Propagation and Dynamic Properties of Earth Materials.* New Mexico: Univ. of New Mexico Press.
Newmark, N. M. and Hall, W. J. 1982. Earthquake spectra and design. EERI Monograph Series, Berkeley, CA.
Newmark, N. M., Blume, J. A. and Kapur, K. K. 1973. Seismic design spectra for nuclear power plants. *J. Power Div. Am. Soc. Civ. Engrs* **99**(PO2): 287–303.
Nuttli, O. W. and Herrman, R. B. 1978. State-of-the-art for assessing earthquake hazards in the United States—Report 12, credible earthquakes for the Central United States. Misc. paper S-73-1. Vicksburg, MS: U.S. Army Corps of Engineers, Waterways Experimental Stations, Geotechnical Lab.
O'Roark, T. D. et al. 1984. *Guidelines for Tunnel Lining Design.* New York: ASCE.
O'Rourke, M. and Wang, L. R. L. 1978. Earthquake response of buried pipeline. Paper presented at ASCE Geotechnical Eng. Div. Specialty Conf., Pasadena, CA.
Okamoto, S. and Tamura, C. 1973. Behavior of subaqueous tunnels during earthquakes. *Earthquake Engineering and Structural Dynamics*, Vol. 1.
Owen, G. N. and Scholl, R. E. 1981. *Earthquake Engineering of Large Underground Structures.* JAB-7821. San Francisco: URS/John A. Blume.
Owen, G. N., Scholl, R. E. and Brekke, T. L. 1979. Earthquake engineering of tunnels. *Proc. Rapid Excavation and Tunneling Conf., Atlanta,* pp. 709–721. New York: Am. Inst. of Mining, Metallurgical, and Petroleum Engrs.
Parsons Brinckerhoff, 1960. Trans-Bay Tube. Technical Supplement to the Engineering Report, Bay Area Rapid Transit District, San Francisco.
Peck, R. B., Hendron, A. J. and Mohraz, B. 1972. State of the Art of Soft Ground Tunneling. *Proc. Rapid Excavation and Tunneling Conf.,* pp. 259–286. New York: Am. Inst. of Mining, Metallurgical, and Petroleum Engrs.
Pratt, H. R., Hustrulid, W. A. and Stephenson, D. E. 1979. Earthquake Damage to Underground Facilities. DP-1513. Aiken, SC: Savannah River Laboratory.
Richart F. et al. 1970. *Vibrations of Soils and Foundations.* Englewood Cliffs, NJ: Prentice-Hall.
Rinehart, J. S. 1960. On fractures caused by explosions and impact. *Col. Sch. Mines Q.* **55**(4).
Rozen, A. 1976. Response of Rock Tunnels to Earthquake Shaking. M.S. thesis, MIT, Cambridge, MA.
Schnabel, P. B. and Seed, H. B. 1973. Accelerations in rock for earthquakes in the Western United States. *Bull. seism. Soc. Am.* **63**(2): 501–516.
Schnabel, P. B. et al. 1972. SHAKE—A computer program for earthquake response analysis of horizontally layered sites. Report No. EERC 72-12. Berkeley: Univ. of Calif.
Seed, H. B. and Idriss, I. M. 1982. Ground motions and soil liquefaction during earthquakes. EERI Monograph Series, Berkeley, CA.
Seed, H. B. et al. 1976. Relationships of maximum acceleration, maximum velocity, distance from source, and local site conditions for moderately strong earthquakes. *Bull. seism. Soc. Am.* **66**(4): 1323–1342.
Slemmons, D. B. 1977. State-of-the-art for assessing earthquake hazards in the United States—Rpt 6, faults and earthquake magnitude. Misc. Paper S-73-1. Vicksburg, MS: U.S. Army Corps of Engineers, Waterways Experimental Stations, Soils and Pavements Lab.
Slemmons, D. B. 1982. Determination of design earthquake magnitudes for microzonation. *Proc. 3rd Int. Earthquake Microzonation Conf., Seattle,* Vol. 1, pp. 119–130.
Stevens, P. R. 1977. A review of the effects of earthquakes on underground mines. Open-File Report 77-313. Reston, VA: U.S. Geological Survey.
Tamura, C. and Okamoto, S. 1975. A study on the earthquake resistant design of subaqueous tunnels, *Proc. 5th European Conf. on Earthquake Engng, Istanbul.*
Tamura, C. and Okamoto, S. 1976. On earthquake resistant design of a submerged tunnel. *Proc. Int. Symp. on Earthquake Structural Engng, Univ. of Missouri, Columbia,* pp. 809–822.
Tsai, N. C. and Housner, G. W. 1970. Calculation of surface motions of a layered half-space. *Bull. seism. Soc. Am.* **60**(5): 1625–1652.
URS/John A. Blume & Assoc. 1976. *Comparative Structural Analysis of Type III Underground Waste Storage Tanks at the Savannah River Plant, Aiken, South Carolina.* San Francisco: John Blume.
Wahi, K. et al. 1980. Numerical simulations of earthquake effects on tunnels for generic nuclear waste repositories. SAI-FR-126. Aiken, SC: The Environ. Transp. Div., E.I. Du Pont de Nemours.
Wang, L. R. L. and O'Rourke, M. J. 1977. State-of-the-art of buried lifeline earthquake engineering. *Proc. Lifeline Earthquake Eng. Specialty Conf., ASCE,* pp. 252–266.
Weidlinger, P. 1977. Behavior of underground lifelines in seismic environment. IR-4. New York: Weidlinger.
Werner, S. D. 1985. Earthquake ground motion considerations for inelastic design of reinforced concrete structures. *Inelastic Response of Concrete Structures* (in preparation). Detroit, MI: American Concrete Institute.

Appendix A— Seismic Environment

(Prepared in collaboration with S. D. Werner)

Causes of Earthquakes

Seismologists typically classify earthquakes according to one of four modes of generation—tectonic, volcanic, collapse, or explosion. Tectonic earthquakes, which are by far the most common, are produced when the rock breaks in response to various geologic forces. Tectonic earthquakes are associated with relative displacement that occurs along faults, which may be created or reactivated during the earthquake. Volcanic earthquakes, as the name implies, accompany volcanic eruptions. Collapse earthquakes accompany events such as landslides or the collapse of roofs of underground caverns or mines. Seismic events analogous to tectonic earthquakes may also occur in deep mines and in open cut excavations. These violent releases of strain energy which are "explosive like" in nature are known as rockbursts. Explosion earthquakes are man-made, and arise from detonation of chemical or nuclear devices.

This appendix deals specifically with tectonic earthquakes, since these are of primary concern during design of underground structures. However, the techniques used to quantify the ground motion are equally applicable to other types of earthquakes.

Plate Tectonics

As noted above, faults play a critical role during tectonic earthquakes. These faults may be related to the local geologic environment or to the global pattern of faults that define the boundaries between relatively stable regions of the earth's surface. According to the theory of plate tectonics, these stable regions, or plates, are moving relative to one another; and it is this movement that results in concentration of earthquakes along the plate boundaries. The boundaries can be classed as spreading zones (where plates are moving apart), shear zones (where plates are sliding past one another), collision zones (where plates collide), or subduction zones (where one plate slides underneath another).

A comparison of the location of reported earthquakes and plate boundaries indicate that there is a marked correlation between the two. Indeed, approx. 90% of the total seismic energy for shallow earthquakes occurs within the subduction zones alone. However, events do occur within plates and these cannot be explained by the theory of plate tectonics. These earthquakes arise from more localized systems of tectonic forces. An example of a significant intraplate earthquake is the New Madrid, Missouri (1811–12), event.

Fault Rupture Process

Once relative movement along a fault is initiated as a result of critical buildup of strain energy in the rock by the tectonic or other forces, it spreads

outward in all directions along the fault surface. The propagation of the rupture front is often irregular, reflecting the variability of rock mass properties and the irregular geometry of the fault surface. The final extent of the fault rupture will depend upon the total strain energy available and how it is dissipated and redistributed during the rupture and relative motion. Although details of this complex process are beyond the scope of this discussion, it is appropriate to note the features of the rupture process that are employed to characterize the ground shaking that will be experienced by adjacent structures. These are the stress drop, the total relative displacement, the fault geometry, and the fault rupture length.

Large-magnitude earthquakes are associated with a large release of energy, which corresponds to a large stress drop and large relative displacement over a large area. The stress drop appears to be correlated with the amplitude of the seismic waves generated, whereas the fault displacement is correlated with duration of ground shaking and distribution of amplitudes. Large relative displacements result in larger amplitudes of low frequency, or long period, waves. Other geometrical features of the faulting, including aspect ratio (length to depth), planarity, and the occurrence of bifurcation, or branching, have a profound effect on the frequency content, duration, and amplitude distribution.

Numerical models have been developed to quantify relationships between the fault rupture process and the resulting characteristics of the ground shaking. Unfortunately, these models are still in the development stage and prediction of the characteristics of tectonic earthquakes and the associated ground motion is based primarily on empiricism. It is established, however, that what is experienced at a particular site as a consequence of an earthquake will depend upon the size of the earthquake, the site geology and location relative to the causative fault, and how the seismic waves propagate through the intervening geologic media.

Wave Propagation in Geologic Media

Two classes of seismic waves result from fault rupture: (1) body waves, which propagate through the interior of the rock; and (2) surface waves, which propagate along or near the ground surface. The principal types of body waves are P-waves (also known as dilatational waves or compressional waves); and S-waves (also known as distortional waves or shear waves). P- and S-waves excite particle motion that is, respectively, parallel to and perpendicular to the direction of propagation. These motions are illustrated in Fig. 14a. The propagation velocities depend upon the material and geometrical properties of the medium. For example, the P-wave velocity, in an infinite, homogeneous, isotropic, and elastic medium, is:

$$C_p = \sqrt{\frac{(1-\nu)\,E}{(1+\nu)(1-2\nu)\,\rho}} \quad .$$

In the same circumstances, S-waves propagate with velocity:

$$C_s = \sqrt{\frac{G}{\rho}} = \sqrt{\frac{E}{2(1+\nu)\,\rho}} \quad .$$

From these relationshps it can be seen that P-waves propagate in an infinite medium at least $\sqrt{2}$ times as fast as S-waves.

The most significant types of surface waves are Rayleigh waves and Love waves. Rayleigh waves induce elliptic retrograde particle motion in a vertical plane, i.e. the vertical and horizontal components of particle motion are contained in the plane of wave propagation. Love waves excite particle motion that is horizontal and predominantly normal to their direction of propagation, and occur in a stratified solid if the S-wave velocity is greater in the lower stratum. These types of waves are illustrated in Fig. 14b. Rayleigh waves propagate at a velocity approaching the S-wave velocity, whereas Love waves propagate at a velocity somewhere between the S-wave velocity of the surface layer and that of the lower stratum. Relative propagation velocities of P- , S- , and Rayleigh waves in a semi-infinite, isotropic, elastic medium are illustrated in Fig. 15. Love waves are not included in that figure because they do not occur in homogeneous media.

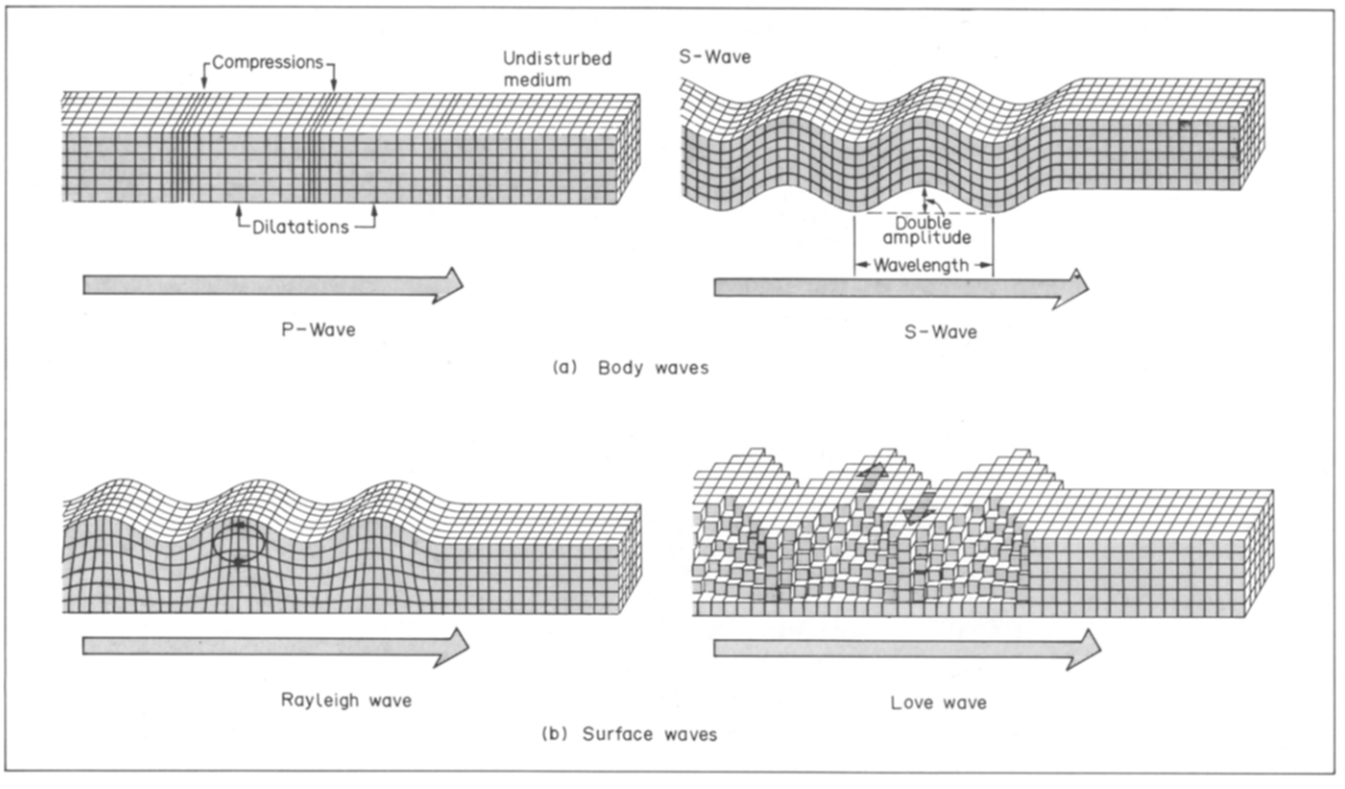

Figure 14. Seismic waves (Bolt 1978).

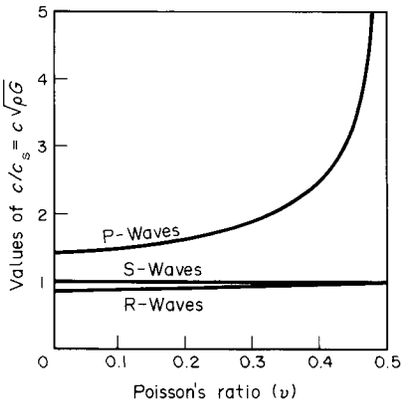

Figure 15. Relation between Poisson's ratio and velocities of propagation of compression (P), shear (S), and Rayleigh (R) waves in a semi-infinite elastic medium (Richart et al. 1970).

The seismic waves that propagate from the source of the site are influenced by the geometry and material properties of the transmission path. Along transmission paths within the subsurface medium, both P- and S-waves are reflected and refracted as they encounter interfaces between layers with different material properties. Interference between reflected and refracted waves can result in a local increase or decrease in amplitudes of the waves as they propagate from the source of energy release. Other irregularities in the transmission path, such as variations in surface topography and discontinuities and inhomogeneities in the subsurface, greatly complicate the reflection and refraction processes. The surface topography and near surface stratigraphy influence the characteristics of surface waves.

In addition to undergoing modifications due to the characteristics of the transmission path, the amplitudes of the seismic waves are modified as a result of geometric spreading effects and attenuation resulting from the dissipative properties of the subsurface soil and rock materials. The nonlinear characteristics of the subsurface materials also affect the dynamic characteristics of those components of ground shaking associated with wavelengths comparable to or shorter than the characteristic dimensions of the various subsurface layers.

Characteristics of Earthquakes and Ground Motion

The characteristics of earthquakes and ground motion pertinent to the development of seismic input criteria are the size of the earthquake and the intensity, frequency content, and the duration of the ground motion. The generally accepted means of defining each of these characteristics for engineering application is summarized below.

Size of the Earthquake

For engineering purposes, the size of an earthquake most typically is represented in terms of the earthquake magnitude. The magnitude is calculated from measurements recorded on seismographs but is, of course, independent of the point of observation. Several different magnitude scales are currently in use, the most common of which are the local magnitude, M_L; the surface wave magnitude, M_S; the body wave magnitude, M_B; and the moment magnitude, M_W. The choice of magnitude measure to be used is governed to a considerable extent by the characteristics of the event itself. The means of defining each and the normal application of each is summarized in Table 4. The relative values of the different magnitude scales are illustrated in Fig. 16.

Physically, the magnitude has been correlated with the energy released by the earthquake, as well as the fault rupture length, felt area, and maximum fault displacement. Several magnitude vs fault rupture length correlations

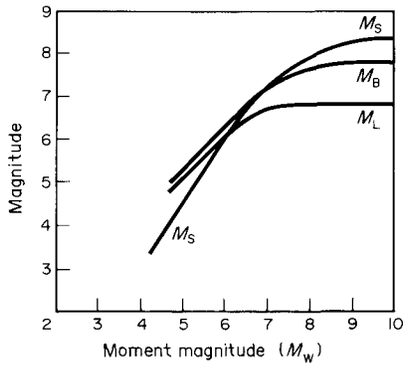

Figure 16. Numerical values (Boore and Joyner 1982).

derived using worldwide data are shown in Fig. 17. Similar curves have been derived for specific areas and specific types of faults. In current engineering applications, such curves are used in estimating design earthquakes. For such estimation, the fault rupture length is usually assumed to be equal to 1/2 or 1/3 of the total length of existing faults (Slemmons 1977).

Intensity of the Ground Motion

Both qualitative and quantitative measures have been used to characterize the intensity of the ground shaking. Qualitative measures are based on observed effects of the earthquake motions on people and on structures and their contents. The various intensity scales, such as the Rossi-Forel and Modified Mercalli scales, are examples of qualitative measures of the ground shaking.

Quantitative measures, on the other hand, correspond to quantities for representing the intensity of the shaking that are obtained directly from ground motion time histories. Typically, a single parameter is used to describe the intensity. Peak acceleration, peak velocity, peak displacement, spectrum intensity, root-mean-square acceleration, and Arias intensity are among the

Table 4. Definition and application (Housner and Jennings 1982).

Magnitude	Definition	Application
Local, M_L	Logarithm of peak amplitude (in microns) measured on Wood–Anderson seismograph at distance of 100 km from source and on firm ground. In practice, corrections made to account for different instrument types, distances, site conditions.	Used to represent size of moderate earthquake. More closely related to damaging ground motion than other magnitude scales.
Surface wave, M_S	Logarithm of maximum amplitude of surface waves with 20-s period.	Used to represent size of large earthquakes.
Body wave, M_b	Logarithm of maximum amplitude of P-waves with 1-s period.	Useful for assessing size of large, deep-focus earthquakes which do not generate strong surface waves.
Moment, M_w	Based on total elastic strain-energy released by fault rupture, which is related to seismic moment M_o ($M_o = G \cdot A \cdot D$, where G = modulus of rigidity of rock, A = area of fault rupture surface, D = average fault displacement).	Avoids difficulty associated with inability of surface wave magnitudes to distinguish between two very large events of different fault lengths (saturation).

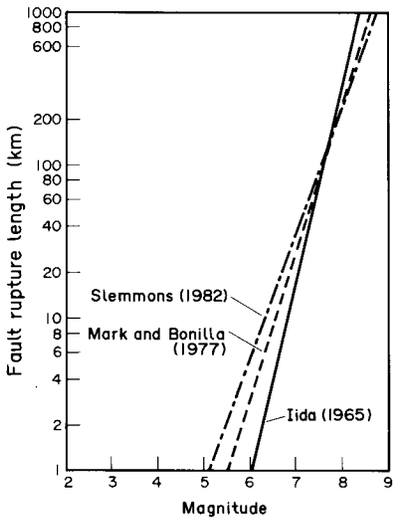

Figure 17. Comparison of recent correlations between fault rupture length and earthquake magnitude.

parameters that have been used for this purpose. Of these, the most widely used measure is the peak ground acceleration. However, it should be remembered that peak ground acceleration is not a good indicator of the damage potential of ground motion, i.e. it is repetitive shaking with strong energy content that leads to structural deformation and damage. As a result, the term "effective acceleration" has been used to refer to an acceleration which is less than the peak free-field acceleration and is more representative of the damage potential of ground motion (Newmark and Hall 1982).

In view of the emphasis on peak ground motion that would be experienced at a site, considerable attention has been devoted to developing attenuation relationships. These are empirical relationships derived from measured free-field data on ground motion strength, duration parameters, magnitude, distance, and, in some instances, site conditions. Not surprisingly, attenuation relationships most commonly have been derived for peak acceleration. However, empirical relationships for peak velocity, peak displacement, and the other single-parameter measures of the intensity of the ground shaking also have been developed. Several relationships for peak acceleration are summarized in Table 5 for illustrative purposes.

Since the empirical attenuation relationships are derived through statistical regression, the form of the equation can vary markedly from one investigator to the next. However, the resulting attenuation curves are, in general, more sensitive to the availability of strong motion data than to the regression equation form.

A comparison of recent peak acceleration vs distance correlations derived using strong motion data is given in Fig. 18. The figure illustrates that the various correlations are in relatively good agreement for earthquakes of magnitude 6.5. The quality of this agreement may be attributed to the large data base for earthquakes of this magnitude. On the other hand, the data base on 7.3 magnitude earthquakes is more limited and the relationships diverge substantially at a distance less than 10 km from the fault. Accordingly, one is led to the conclusion that while such relationships provide a valuable basis for developing seismic design criteria where data are ample, they should be used with caution for conditions where the data are sparse or nonexistent.

Frequency Content of the Ground Motion

To define the frequency content of the ground shaking, a frequency spectrum is required. Two types of spectra are widely used in current earthquake engineering practice. One type is the response spectrum, which is useful because it indicates ground motion frequency characteristics in a form that is of most direct application to structural analysis and design, especially where linear response is to be estimated. The response spectrum is defined as a plot of the maximum response of a single-degree-of-freedom oscillator, as a function of its frequency and damping ratio. This response can be plotted in a

Table 5. Attenuation relationships for peak ground acceleration.

Data source	Magnitude range of data	Distance range of data (km)	Soil factors	Equation	References	Comments
153 records from Western US earthquakes	5-0-7.6	6.0-160	Rock	Graphical	Schnabel and Seed (1973)	Supplemented available data base by computing rock outcrop motions from surface ground motions at 11 structures
Records from Central United States	$\leqq 6.0$		None	$\log A = -0.36 + 0.56\, m_b - 0.00 \log R \quad R \leqq 15$ km $\log A = 0.84 + 0.52\, m_b - 1.02 \log R \quad R \geqq 15$ km where A = peak acceleration, cm/s^2 m_b = body wave magnitude R = epicentral distance, km	Nuttli and Herrmann (1978)	Relations based in part upon theoretical formulations, and in part upon observational data.
70 records from United States	4.4-7.7	10-250	Rock Soil	$\ln A = 3.40 + 0.89M\ 1.17 \ln R - 0.20\, Y_s$ where A = peak acceleration magnitude M = earthquake magnitude R hypocentral distance, km $Y_s = \begin{cases} 0 \text{ Rock} \\ 1 \text{ Soil sites} \end{cases}$	McGuire (1978)	Used both horizontal components of each record.
116 records from 27 earthquakes world wide	5.0-7.7	<50	None	$A = 0.0159\, e^{0.868M} [R + 0.0606\, e^{0.700M}]^{-1.09}$ where A = peak acceleration, g M = Richter magnitude R = distance to causative fault	Campbell (1981)	Used records with peak acceleration of at least 0.02 g for one component. Used both horizontal components of each record.
182 records from 23 earthquakes in Western North America	5.0-7.7	4.0-300	None	$\log A = -1.02 + 0.249M - \log r - 0.00255r$ where A = peak acceleration, g M = moment magnitude $r = (R^2 + 7.3^2)^{1/2}$ R = Distance to fault, km	Joyner and Boore (1981)	Used the larger of the two horizontal components.

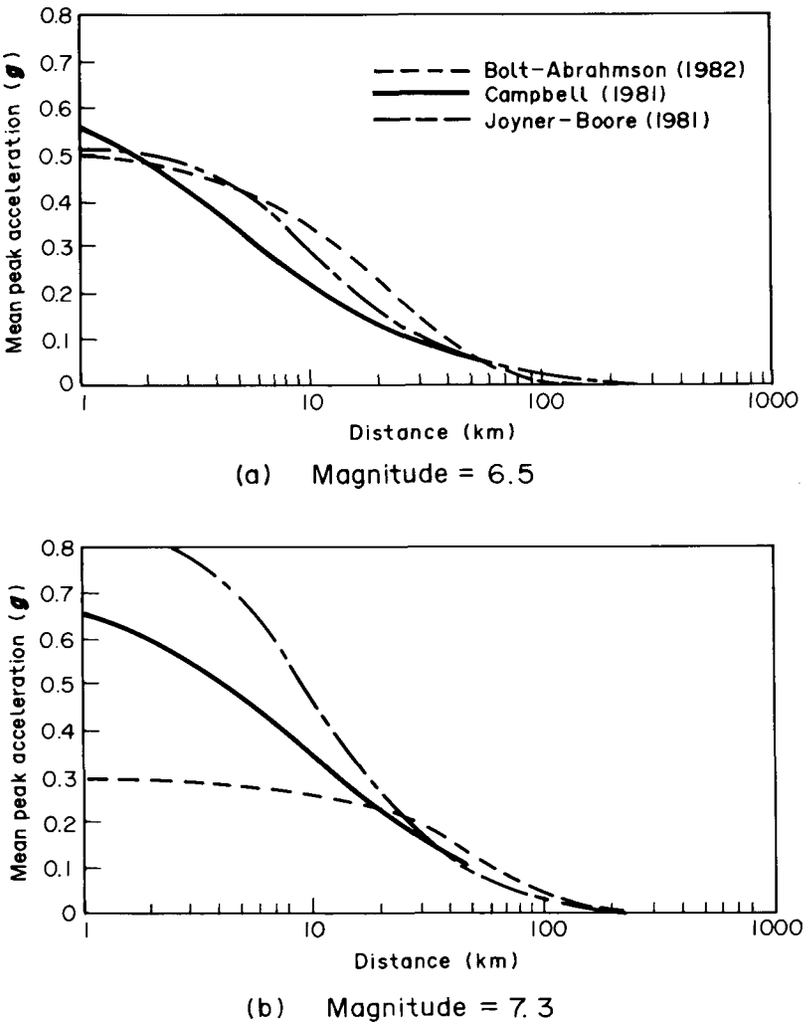

Figure 18. Comparison of recent correlations between horizontal peak acceleration, magnitude and distance (modified from Donovan 1982).

linear form or in the more familiar logarithmic, tripartite form. An illustration of this type of response spectrum is provided in Fig. 19.

The second principal type of frequency spectrum is the Fourier Amplitude spectrum, which is defined as a plot of the amplitude of the relative velocity for an undamped single-degree-of-freedom oscillator at the end of the record as a function of its frequency. Such spectra have been used in studies of ground shaking and strong motion seismology for site amplification studies at strong motion accelerometer stations, evaluations of wave transmission characteristics recorded by differential arrays of accelerographs, and source mechanism studies. They are not considered further in this text.

Duration of Strong Motion

In addition to the strength and frequency content of the ground shaking, the duration of strong shaking will influence the effects of the earthquake motion on the response of structures. In particular, the number of excursions of the structure into the nonlinear range is likely to control the extent of permanent damage. Unfortunately, there is, at present, no single universally accepted approach for quantifying the duration of strong shaking for a given ground motion accelerogram. Several approaches, including specifying the time between the first and last excursions of ground acceleration above some specified level, have been proposed; however, these have not yet been developed to a point where they can be incorporated into routine seismic design criteria.

Specifications of Seismic Input Criteria

At present, the most widely used approach for specifying seismic input criteria for surface structures is through development of response spectra. Two

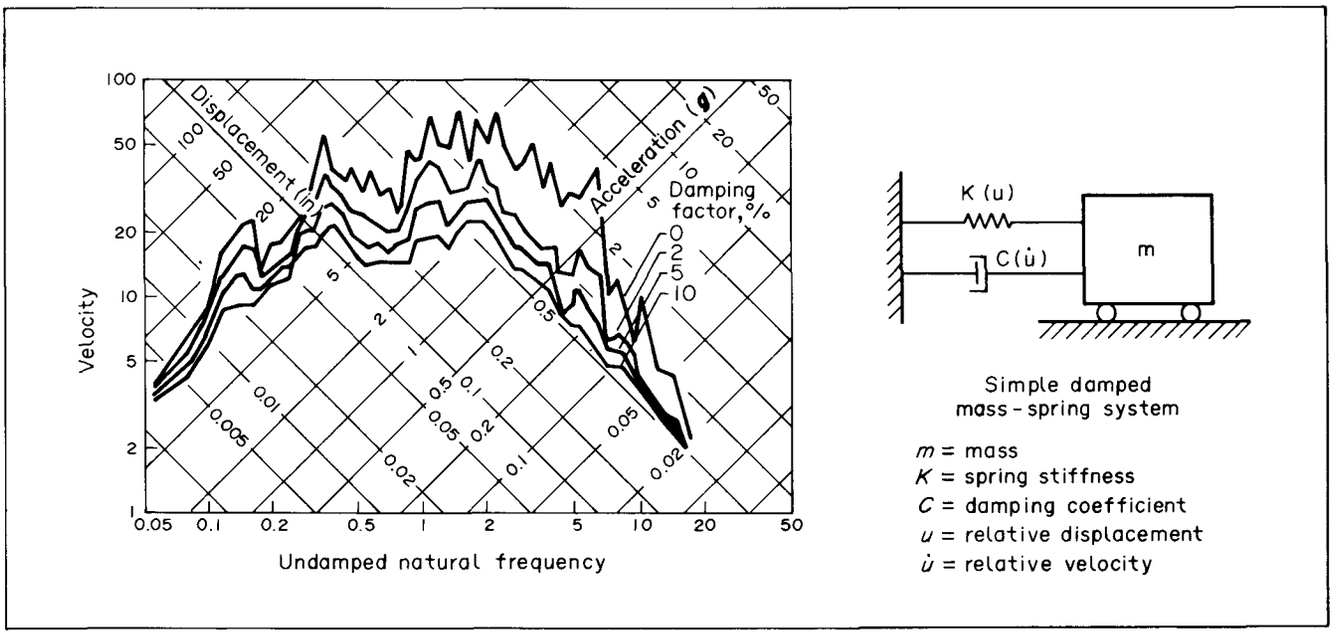

Figure 19. Maximum response of a simple damped oscillator to dynamic motion of its base.

aspects of this approach for defining seismic design criteria should be noted. First, the response spectra should be representative, not only of the anticipated characteristics of the ground motion at the site, but also of an acceptable level of structural response. Second, a response spectrum approach should not be used if (1) the structure's response is highly nonlinear; or (2) the structure is sufficiently long that earthquake input motion could vary significantly in amplitude and phase along its length. In these cases, the specification of seismic input criteria in the form of motion time-histories is most appropriate. Definition and use of motion time-histories for design/analysis of underground excavations are discussed in the main text, under "Seismic Activity." The discussion here is more relevant for free-standing structures, either on the surface or within underground excavation, and serves primarily to illustrate an alternative approach to definition of seismic input criteria.

The two approaches currently in use for developing response spectra—deterministic and probabilistic—differ in the method used to account for the various uncertainties associated with the earthquake process. The most important uncertainties are the timing and location of future earthquakes of a given size and the characteristics of the resultant ground shaking that would be experienced at a particular site.

Deterministic Approach

Deterministic methods do not directly account for the uncertainties in the occurrence of earthquakes. Instead, specific earthquake events associated with particular faults or other geologic features are identified, and the sizes (magnitudes, epicentral intensities, etc.) and source-site distances associated with these events are used for the development of the response spectra. Standard ground motion vs distance attenuation curves derived from statistical regression analyses are used to establish the general levels of shaking at the site. These ground shaking levels are then used to derive response spectra by scaling standardized spectrum shapes.

Standardized spectrum shapes are developed from statistical analysis of response spectra with different levels of damping for an ensemble of measured ground motion records, either for a variety of geologic settings or one specific type of geologic setting. An example of a general response spectrum is given in Fig. 20. That particular spectrum was adopted by the Nuclear Regulatory Commission as a standard for design of nuclear facilities.

Site-dependent spectra are developed by grouping ground motion records according to local site geology. Examples of such spectrum shapes, which are incorporated in the ATC-3 provisions for the development of seismic regulations for buildings, are reproduced in Fig. 21.

Probabilistic Approach

Probabilistic methods differ from deterministic methods in that they use simple probabilistic models as tools for estimating effects of uncertainties in the occurrence of earthquakes and in the attenuation relationships. The occurrence of earthquake events in time and space within each potential earthquake source is represented using a simple probabilistic model. Most commonly, it is assumed that future earthquake events are spatially and temporally independent. Accordingly, it is often assumed that the future occurrence of seismic events in time can be described as a homogeneous Poisson process with a uniform occurrence rate. Also, the spatial distribution of earthquakes in a particular source zone is almost always assumed uniform, although any number of such zones can be defined as a basis for probabilistically modeling the ground shaking. In general, earthquake magnitudes are considered to be exponentially distributed. When coupled with applicable ground motion attenuation relationships, this approach leads to definition of the probability of exceeding a given level of ground shaking at the site.

In its simplest form, the current practice is, typically, to use peak ground acceleration as the single measure of the strength of shaking at the site. Peak

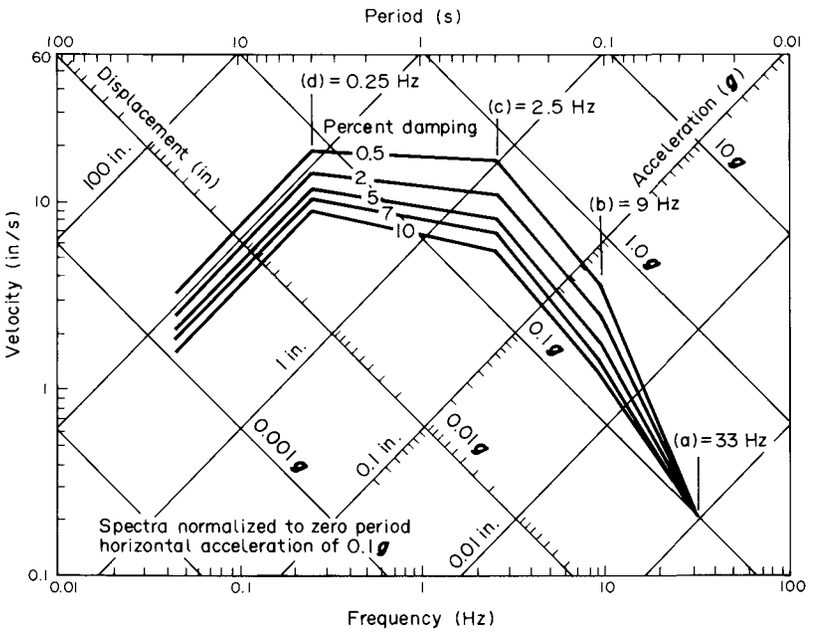

Figure 20. Site-independent spectrum shapes: horizontal motion, RG 1.60 (Newmark et al. 1973).

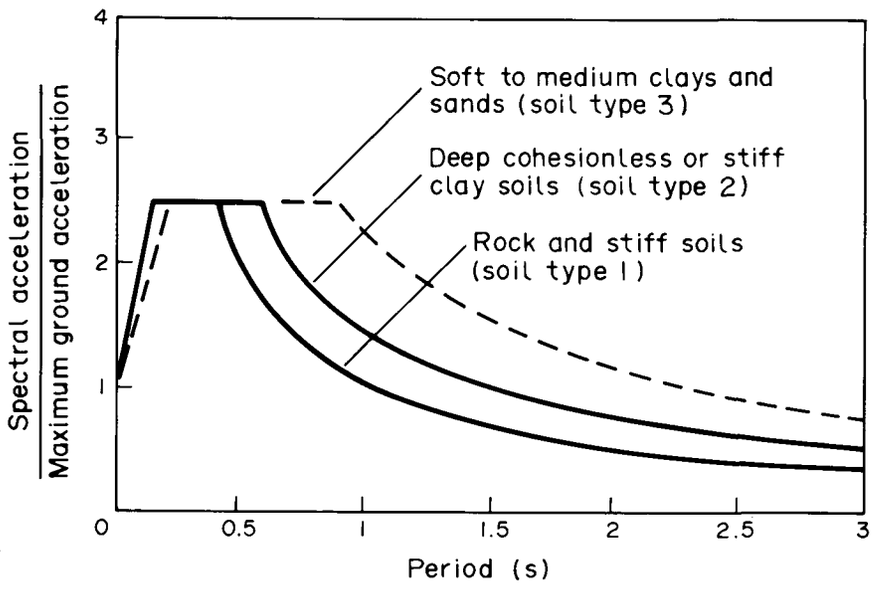

Figure 21. Site-dependent spectrum shapes in ATC-3 (1978) seismic design provisions.

acceleration vs probability curves are developed and are entered at a selected probability level in order to define the peak ground acceleration. This acceleration is then used to scale a fixed spectrum shape (which may be site-independent or site-dependent) in order to obtain the site design response spectra. This approach is summarized schematically in Fig. 22. However, because the use of fixed spectrum shapes has certain limitations, some investigators have developed procedures for probabilistically defining the spectral amplitudes of the design spectrum on a frequency-by-frequency basis. Although this approach would appear to be more refined than the fixed spectrum shape approach, it does require frequency-dependent attenuation data, which often are not really available.

Appendix B— Theoretical Development of Seismic Response When Ground/Structure Interaction Is Ignored

This appendix provides a detailed description of the assumptions made to arrive at the recommended preliminary design procedure for structures in soil and rock summarized under "Recommended Procedures for Preliminary Design of Underground Structures." Although part of this appendix overlaps the material presented under "Structures that Conform to Ground Motion," it is included here for clarity and ease of reference.

As discussed previously, the analytical method for estimating the strains and stresses experienced by an underground structure when it conforms to ground motion is based on the theory of wave propagation in an infinite, homogeneous, isotropic, elastic medium. The case is pertinent to most tunnels in rock and many soils, since the liner stiffness is low in comparison to that of the medium.

Seismic Strains

The particle motion associated with a plane wave propagation in the x-direction in an infinite medium can be represented by

$$u(x,t) = f(x-ct) \tag{B-1}$$

where t represents time and c, the apparent wave propagation velocity.

The first and second derivatives of the displacement function with respect to location in time, t, and space, x, are

$$\frac{\partial u}{\partial x} = f'(x-ct) \qquad \frac{\partial^2 u}{\partial x^2} = f''(x-ct) \tag{B-2}$$

$$\frac{\partial u}{\partial t} = -c\,f'(x-ct) \qquad \frac{\partial^2 u}{\partial t^2} = c^2 f''(x-ct) \; .$$

From the above expressions, the following relationships can be derived

$$\frac{\partial u}{\partial x} = -\frac{1}{c}\frac{\partial u}{\partial t} \tag{B-3a}$$

and

$$\frac{\partial^2 u}{\partial x^2} = \frac{1}{c^2}\frac{\partial^2 u}{\partial t^2} \tag{B-3b}$$

where $\frac{\partial u}{\partial x}$ is a measure of strain; $\frac{\partial^2 u}{\partial x^2}$ represents the curvature; and $\frac{\partial u}{\partial t}$ and $\frac{\partial^2 u}{\partial t^2}$ represent, respectively, the particle velocity and acceleration. In the special case where the displacement function can be assumed as a sine or cosine function

$$u = u_m \sin\frac{2\pi}{L}(x-ct) \tag{B-4}$$

where L is the wavelength and u_m the maximum displacement amplitude, Equation (B-3b) yields

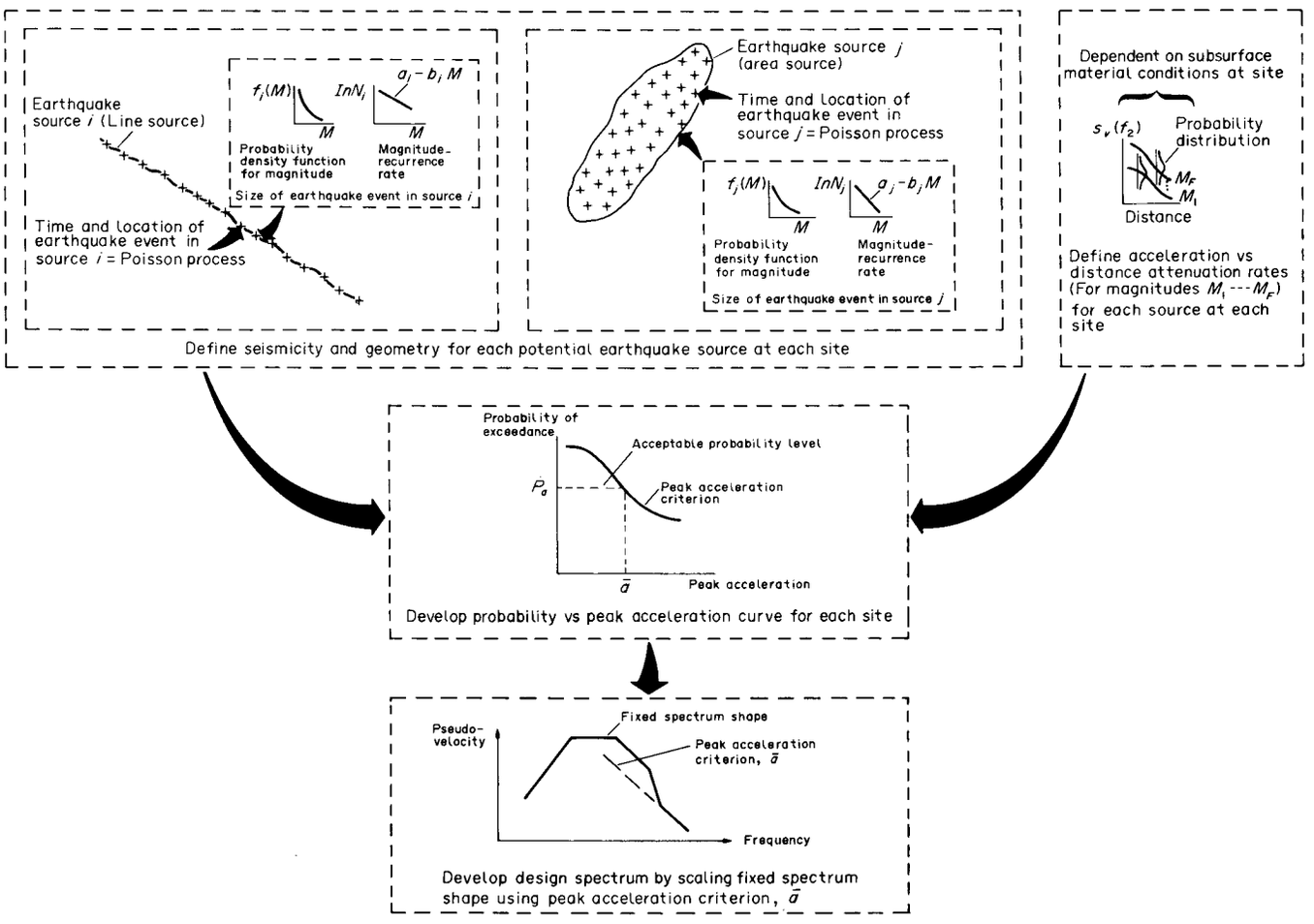

Figure 22. Current practice for carrying out seismic hazard assessment in terms of peak acceleration.

$$u_m\left(\frac{2\pi}{L}\right)^2 = \frac{1}{c^2}\frac{\partial^2 u}{\partial t^2} \quad . \tag{B-5}$$

With the maximum particle acceleration defined as a_m, the maximum displacement amplitude is given by

$$u_m = \left(\frac{L}{2\pi c}\right)^2 a_m = \left(\frac{T}{2\pi}\right)^2 a_m \tag{B-6}$$

where T represents the period of the wave. Of course, the above equation is valid only for a sinusoidal wave.

For a P-wave, the particle motion is in the direction of wave propagation (Fig. 14) and, as a result, the axial or longitudinal strain is given by

$$\epsilon_l = \pm \frac{\partial u_l}{\partial l} \quad . \tag{B-7}$$

The axial strain can be related to the particle velocity of the soil (Equation (B-3a)) as follows:

$$\epsilon_l = \pm \frac{1}{c_p}\frac{\partial u_l}{\partial t} = \pm \frac{1}{c_p}\dot{u}_l \tag{B-8}$$

where c_p represents the P-wave velocity. By setting the maximum particle velocity due to P-wave equal to V_p, the maximum axial strain will be given by

$$\epsilon_{l_m} = \pm \frac{V_p}{C_p} \quad . \tag{B-9}$$

The strain normal to the x-axis and the shear strain are zero because of the assumed nature of the wave.

For a shear wave, the particle motion is in the direction perpendicular to that of wave propagation (Fig. 14) and, as a result, the shear strain is given by

$$\gamma = \frac{\partial u_n}{\partial l} \quad . \tag{B-10}$$

The shear strain can be related to the particle velocity of the soil as follows:

$$\gamma = \pm \frac{1}{c_s}\frac{\partial u_n}{\partial t} = \pm \frac{1}{c_s}\dot{u}_n \tag{B-11}$$

where c_s represents the apparent S-wave velocity. By setting the maximum particle velocity equal to V_s, the maximum shear strain will be given by

$$\gamma_m = \frac{V_s}{c_s} \quad . \tag{B-12}$$

In this case, the longitudinal and normal strains are zero.

In addition, a shear wave gives rise to a curvature along the direction of wave propagation, which can be defined (Equation (B-3b)) as:

$$\frac{1}{\rho} = \frac{1}{c_s^2}\frac{\partial^2 u_n}{\partial t^2} = \frac{1}{c_s^2}\ddot{u}_n \quad . \tag{B-13}$$

By setting the maximum particle acceleration due to shear wave equal to a_s, the maximum curvature will be given by

$$\frac{1}{\rho} = \frac{a_s}{c_s^2} \quad . \tag{B-14}$$

Finally, a P- or S-wave propagating at an angle ϕ to the axis of the structure will cause longitudinal, normal and shear strains, which are summarized in Table 1. The curvature along the axis of the structure is also given in the table. Each of these quantities can be maximized by adjusting the value of the angle of incidence, ϕ. The maximum value for each quantity is shown in Table 1.

The strains experienced by the tunnel structure can be easily calculated if the structure is treated as a simple beam. The design strains and curvatures are given directly by Table 1. The combined longitudinal strain from axial deformation and bending is also of interest. This strain is given by

$$\epsilon_{ap} = \frac{V_p}{c_p}\cos^2\phi + \frac{Ra_p}{c_p^2}\sin\phi\cos^2\phi \tag{B-15a}$$

for a P-wave, and by

$$\epsilon_{as} = \frac{V_s}{c_s}\sin\phi\cos\phi + \frac{Ra_s}{c_s^2}\cos^3\phi \tag{B-15b}$$

for an S-wave, where R represents the distance from the neutral axis to the extreme fiber of the tunnel cross-section. It is apparent from the above expressions that the maximum value for the axial strain and bending strain occur at different values of the angle of incidence and, as a result, the value of ϕ that will maximize the longitudinal strain varies, depending on the dimension of the structure. An upper limit to the combined longitudinal strain is given by the sum of the maximum of each of the axial and bending strain, i.e.

$$\epsilon_{pm} = \frac{V_p}{c_p} + 0.385\,\frac{Ra_p}{c_p^2} \quad ; \tag{B-16a}$$

$\phi =$ 0° axial strain
35° 16′ bending strain

for a P-wave where i, and

$$\epsilon_{sm} = \frac{V_s}{2c_s} + \frac{Ra_s}{c_s^2} \quad ; \tag{B-16b}$$

$\phi =$ 45° axial strain
0° bending strain

for an S-wave. Noting that

$$c_p = \sqrt{\frac{2(1-\nu)}{(1-2\nu)}}\,c_s \tag{B-17}$$

it can be easily shown that, in a medium with a Poisson's ratio smaller than 0.33, the maximum axial strain is due to a compressional wave if it is assumed that the particle velocities due to P- and S-waves are equal. The bending strain is usually much smaller than the axial strain. As a result, the upper limit for the combined longitudinal strain is, in general, due to a compressional wave.

Seismic Stresses

Once the strains have been evaluated, the stresses in the medium around the tunnel structure can be estimated by using the three-dimensional constitutive relations for a linear, elastic, isotropic material; namely,

$$\sigma_x = \frac{E}{(1+\nu)(1-2\nu)}[(1-\nu)\,\epsilon_x + \nu(\epsilon_y + \epsilon_z)] \tag{B-18a}$$

and

$$\tau_{xy} = G\,\gamma_{xy} \quad . \tag{B-18b}$$

in which σ_x and τ_{xy} are, respectively, normal and shear stress; and E, G, and ν—the elastic modulus, shear modulus, and Poisson's ratio of the medium. The maximum stresses in the medium due to body waves along with the angle of incidence for the wave are summarized in Table 2. These values were found as follows.

For a P-wave, the strain components for a wave propagating parallel to the axis of the tunnel are (from Table 1).

$$\epsilon_x = \frac{V_p}{C_p}$$

$$\epsilon_y = \epsilon_z = 0 \quad . \tag{B-19}$$

From Equation (B-18a), the normal stress is given by

$$\sigma_p = \frac{(1-\nu)\,E}{(1+\nu)(1-2\nu)}\frac{V_p}{c_p} \quad . \tag{B-20}$$

The maximum shear stress is obtained for a wave traveling at 45 deg. to the axis of the structure and is given by

$$\tau_p = G\frac{V_p}{2c_p} \quad . \tag{B-21}$$

For a shear wave, the maximum normal stress is obtained for a wave propagating

at 45 deg. to the axis of the structure. In this case, the strains are equal to

$$\epsilon_x = \epsilon_y = \frac{V_s}{2c_s} \qquad \text{(B-22)}$$

$$\epsilon_z = 0 \quad .$$

The maximum normal stress is thus given by

$$\sigma_s = \frac{E}{(1+\nu)(1-2\nu)} \frac{V_s}{2c_s} \quad . \qquad \text{(B-23)}$$

The maximum shear stress is obtained when the wave is traveling parallel to the axis of the structure and is given by

$$\tau_s = G \frac{V_s}{c_s} \quad . \qquad \text{(B-24)}$$

It is interesting to know that for a medium with a Poisson's ratio greater or equal to 0.19, the maximum normal stress in that medium is due to a shear wave rather than a compressional wave. In the above conclusion, the particle velocity due to P-wave and that due to S-wave are assumed to be equal. The maximum shear stress is also due to a shear wave.

The maximum stresses in the medium resulting from P- and S-waves are summarized in Table 2. These are, of course, the free-field stresses that would be used as boundary conditions if simple continuum models are to be used for design of lined or unlined tunnels. If, instead, the tunnel structure is treated as a simple beam, then the stresses are obtained by using the equations from beam theory and the strains and curvature given in Table 1. Namely, the axial stresses are given by the relation

$$\sigma_a = E' \epsilon$$

where ϵ is the axial or longitudinal strain and E is the elastic modulus of the tunnel section material, and the bending stresses are given by

$$\sigma_b = \frac{E' R}{\rho}$$

where R is the distance from the neutral axis of the tunnel section and ρ is the radius of curvature. For example, for a shear wave the maximum axial stress is given by

$$\sigma_a = E' \epsilon_s = \frac{E' V_s}{2c_s} \qquad \text{(B-25)}$$

and the maximum bending stress is given by

$$\sigma_b = \frac{E' R}{\rho} = \frac{E' R a_s}{c_s^2} \quad . \qquad \text{(B-26)}$$

The upper limit for the longitudinal stress is given by the sum of the maximum for the axial and bending stresses. This approach is conservative because the maxima do not occur at the same time.

Appendix C— Theoretical Development of Seismic Response When Ground/Structure Interaction is Considered

This appendix provides a detailed description of the assumptions made to arrive at the recommended preliminary design procedure for subaqueous tunnels summarized in the above text. Part of this appendix overlaps the material presented in the text, but is included for completeness, clarity and ease of reference.

As discussed in the text, the analytical procedure for estimating the forces experienced by structures that do not conform to the ground motion during seismic excitation is based on the theory of wave propagation in an infinite, homogeneous, isotropic, elastic medium, and the theory for an elastic beam on an elastic foundation. The equations for wave propagation are used to determine the free ground deformations or the ground deformations in the absence of the tunnel structure. Since the tunnel structure is stiffer than the surrounding soil, the structure will not conform to the free ground deformations.

The beam theory is necessary to account for the effects of interaction between the soil and the tunnel structure. This approach parallels, in part, the procedure developed for the design of the Trans-Bay Tube for the San Francisco Bay Area Rapid Transit (Parsons Brinckerhoff 1960), and the work of several investigators (Kuribayashi et al. 1975, 1977).

The following discussion develops the procedure outlined above. The effects of, first, transverse horizontal shear waves and, subsequently, vertical shear waves and compressional waves are considered; then the equations needed to estimate the forces acting on a subaqueous tunnel structure during an earthquake excitation are derived.

Forces Due to Transverse-Horizontal Shear Waves

A tunnel structure subjected to an incident sinusoidal shear wave with a wavelength L and amplitude A, as shown in Fig. 11 in the main text, will experience a transverse displacement,

$$u_y = A \cos \phi \sin \frac{2\pi x}{L/\cos \phi} \qquad \text{(C-1)}$$

and an axial displacement,

$$u_x = A \sin \phi \sin \frac{2\pi x}{L/\cos \phi} \qquad \text{(C-2)}$$

where ϕ is the angle of incidence between the direction of wave propagation and the axis of the structure. Assuming the structure behaves like a beam, the curvature due to transverse displacements is given by

$$\frac{1}{\rho} = \frac{\partial^2 u_y}{\partial x^2} = -\left(\frac{2\pi}{L}\right)^2 \cos^3 \phi \, A \sin\left(\frac{2\pi x}{L/\cos \phi}\right) \qquad \text{(C-3)}$$

where ρ is the radius of curvature. The resulting forces in the tunnel structure are:

(a) a bending moment,

$$M = \frac{E'I}{P} = \left(\frac{2\pi}{L}\right)^2 \cos^3 \phi \, E'I \, A \sin\left(\frac{2\pi x}{L/\cos \phi}\right) \qquad \text{(C-4)}$$

(b) a shear force,

$$V = \frac{\partial M}{\partial x} = \left(\frac{2\pi}{L}\right)^3 \cos^4 \phi \, E'I \, A \cos\left(\frac{2\pi x}{L/\cos \phi}\right) \qquad \text{(C-5)}$$

(c) an equivalent load density (load per unit length) necessary to cause the curvature,

$$P = \frac{\partial V}{\partial x} = \left(\frac{2\pi}{L}\right)^4 \cos^5 \phi \, E'I \, A \sin\left(\frac{2\pi x}{L/\cos \phi}\right) \qquad \text{(C-6)}$$

and (d) an axial force,

$$Q = \left(\frac{2\pi}{L}\right) \sin \phi \cos \phi \, E'A_c \, A \cos\left(\frac{2\pi x}{L/\cos \phi}\right) \qquad \text{(C-7)}$$

where E', I, and A_c represent, respectively, the elastic modulus, the moment of inertia, and the cross-sectional area of the tunnel structure.

These forces and bending moments are experienced by the tunnel structure if, as assumed, there is no soil/structure interaction. However, we are considering the case when the structure is stiffer than the surrounding medium. Accordingly, it will distort less than the free ground deformations and there will be interaction between the tunnel structure and the surrounding medium. This interaction can be taken into account if it is assumed that the tunnel structure behaves as an elastic beam supported on elastic foundation. In that

case, the differential equation for the tunnel structure can be written as

$$E'I \frac{d^4 u_t}{dx^4} = P \qquad \text{(C-8)}$$

where u_t represents the actual displacement of the structure and P represents the pressure between the structure and surrounding soil. If it is assumed that the soil provides a support that can be idealized as a series of linear elastic springs, then the pressure P can be written as

$$P = K_h (u_y - u_t) \qquad \text{(C-9)}$$

where K_h corresponds to the transverse horizontal foundation modulus of the surrounding medium, and is equal to the spring constant per unit length of the structure. The differential equation for the beam structure is, therefore

$$E'I \frac{\partial^4 u_t}{\partial x^4} + K_h u_t = K_h u_y \quad . \qquad \text{(C-10)}$$

The curvature of the tunnel structure obtained by solving the above equation is smaller than the curvature given by Equation (C-3) by a factor

$$R_1 = \frac{1}{1 + \frac{E'I}{K_h}\left(\frac{2\pi}{L}\right)^4 \cos^4 \phi} \quad . \qquad \text{(C-11)}$$

The forces to which the tunnel structure is subjected can be obtained by multiplying Equations (C-4–C-6) by the above reduction factor. The bending moment in the structure is thus given by

$$M = \frac{\left(\frac{2\pi}{L}\right)^2 \cos^3 \phi}{1 + \frac{E'I}{K_h}\left(\frac{2\pi}{L}\right)^4 \cos^4 \phi} \; E'I\,A \sin\left(\frac{2\pi x}{L/\cos\phi}\right) \qquad \text{(C-12)}$$

the shear force, by

$$V = \frac{\left(\frac{2\pi}{L}\right)^3 \cos^4 \phi}{1 + \frac{E'I}{K_h}\left(\frac{2\pi}{L}\right)^4 \cos^4 \phi} \; E'I\,A \cos\left(\frac{2\pi x}{L/\cos\phi}\right) \qquad \text{(C-13)}$$

and the pressure between the structure and surrounding soil, by

$$P = \frac{\left(\frac{2\pi}{L}\right)^4 \cos^5 \phi}{1 + \frac{E'I}{K_h}\left(\frac{2\pi}{L}\right)^4 \cos^4 \phi} \; E'I\,A \sin\left(\frac{2\pi x}{L/\cos\phi}\right) \quad . \qquad \text{(C-14)}$$

The same approach can be used to derive the expression for the axial force. In this case, the governing differential equation is

$$E'A_c \frac{d^2 u_a}{dx^2} = + K_a (u_a - u_x) \qquad \text{(C-15)}$$

where u_a is the actual axial deformation of tunnel structure and K_a corresponds to the axial foundation modulus of the surrounding medium. The axial deformation given by Equation (C-2) should be reduced by the factor R_2 given by

$$R_2 = \frac{1}{1 + \frac{E'A_c}{K_a}\left(\frac{2\pi}{L}\right)^2 \cos^2 \phi} \qquad \text{(C-16)}$$

which is obtained by solving the above differential equation. The axial force experienced by the tunnel structure is, therefore,

$$Q = \frac{\left(\frac{2\pi}{L}\right) \sin\phi \cos\phi}{1 + \frac{E'A_c}{K_a}\left(\frac{2\pi}{L}\right)^2 \cos^2 \phi} \; E'A_c\,A \cos\left(\frac{2\pi x}{L/\cos\phi}\right) \qquad \text{(C-17)}$$

which is obtained by reducing the axial force given by Equation (C-7) by the factor R_2.

The design forces are obtained by maximizing the expressions for bending moment, shear force, pressure, and axial force with respect to (a) location along the tunnel structure; (b) the angle of incidence, ϕ; and (c) the wavelength, L. The first condition is met by setting $\sin\left(\frac{2\pi x}{L/\cos\phi}\right)$ and $\cos\left(\frac{2\pi x}{L/\cos\phi}\right)$ equal to unity.

The second condition is met by setting the partial derivatives of Equations (C-12–C-14, C-17) with respect to ϕ equal to zero. The value of ϕ that will maximize the value of the bending moment, shear force, and pressure is zero, which corresponds to a wave parallel to the axis of the tunnel structure. There is no value for ϕ that will maximize the value of the axial force and which is independent of the properties of the structure and surrounding soil medium. It is recommended that an angle of incidence of 45 deg. be used in design. This value of ϕ will maximize the value of the axial force when the soil/structure interaction is neglected (Equation (C-6)). The maximum forces are, thus, given by

$$M_m = \frac{\left(\frac{2\pi}{L}\right)^2}{1 + \frac{E'I}{K_h}\left(\frac{2\pi}{L}\right)^4} E'I.A \qquad \text{(C-18)}$$

$$V_m = \frac{\left(\frac{2\pi}{L}\right)^3}{1 + \frac{E'I}{K_h}\left(\frac{2\pi}{L}\right)^4} E'I.A \qquad \text{(C-19)}$$

$$P_m = \frac{\left(\frac{2\pi}{L}\right)^4}{1 + \frac{E'I}{K_h}\left(\frac{2\pi}{L}\right)^4} E'I.A \qquad \text{(C-20)}$$

$$Q_m = \frac{\left(\frac{2\pi}{L}\right)}{2 + \frac{E'A_c}{K_a}\left(\frac{2\pi}{L}\right)^2} E'A_c.A \quad . \qquad \text{(C-21)}$$

As noted above, Equations (C-18–C-21) need to be maximized with respect to the wavelength, L. Before this step can be taken, the expressions for the foundation moduli, K_h and K_a need to be defined. The process of definition requires some explanation because both depend on the wavelengths of the ground motion to which the structure is subjected.

Foundation Moduli Under Horizontal Load

The foundation modulus is defined as the ratio of the pressure between the tunnel structure and surrounding medium and the reduced displacement in the medium when the tunnel structure is present, Equation (C-9). To arrive at an estimate for the foundation moduli, the two-dimensional, plane-strain solution to the Kelvin's problem is used. Kelvin's problem is an example of a singular solution in elasto-statics of a concentrated force at a point in an infinite, homogeneous, isotropic, elastic medium. This problem is illustrated in Fig. 23. The equation defining the vertical displacement u_y, along the X-axis due to a vertical concentrated load σ_y, can be written as

$$u_y = -\frac{(3 - 4\nu)}{4\pi(1 - \nu)} \frac{\sigma_y}{2G} \ln x \qquad \text{(C-22)}$$

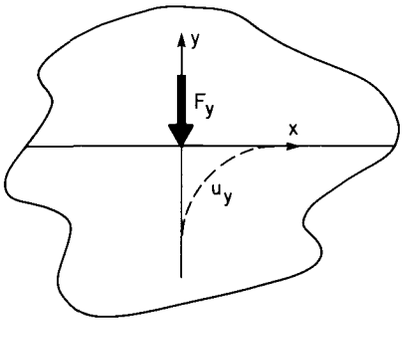

Figure 23. Kelvin's problem: a point force F_y applied within an infinite elastic region induces displacement u_y.

where G and ν represent, respectively, the shear modulus and Poisson's ratio of the elastic medium.

In the present application, the solution corresponding to a sinusoidal load in an infinite elastic medium is sought. Since no closed-form solution to this problem exists, a numerical procedure should be used. The procedure involves, first, deriving the solution to the case of a constant pressure applied to a finite strip in an infinite body. The solution for a sinusoidal distribution of loading then can be found by dividing the wavelength into several segments and assuming the pressure on each segment to be constant. In the present case, this procedure is applied to calculate the displacements under a sinusoidal line load. Each wavelength was divided in 10 and 20 segments and a line load of 4, 6, 8 and 10 wavelengths were considered. It was found that the calculated displacements became insensitive to the number of wavelengths when the latter exceeded 6, and that 10 segments were enough to represent each wavelength.

As a result of this analysis, the vertical displacement under a sinusoidal load may be approximated by

$$u_y = \frac{(3 - 4\nu)}{16\pi\,(1-\nu)G}\,\sigma\,L\,\sin\frac{2\pi x}{L} \qquad \text{(C-23)}$$

where σ represents the maximum amplitude of the pressure. For a tunnel structure with width d and subjected to a horizontal shear wave, the pressure may be defined as the load per unit length over the width of the tunnel structure, or

$$\sigma = \frac{P}{d} \quad . \qquad \text{(C-24)}$$

Substitution of the above equation in Equation (C-23) yields a maximum amplitude for the displacement given by

$$u_{ym} = \frac{(3 - 4\nu)}{16\pi G(1-\nu)}\,P\,\frac{L}{d} \qquad \text{(C-25)}$$

from which the foundation modulus can be defined as follows,

$$K_h = \frac{P}{u_{ym}} = \frac{16\pi G(1-\nu)}{(3 - 4\nu)}\,\frac{d}{L} \quad . \qquad \text{(C-26)}$$

This expression for the foundation modulus is consistent with the derivation of Biot (1965) for the case of an incompressible material.

The procedure described for the case of a vertical sinusoidal load applies for the case of an axial sinusoidal load. It yields the same value for the foundation moduli of the soil medium in both axial and transverse horizontal directions, i.e. $K_a = K_h$.

The above expression for the foundation modulus can be written in a more convenient form:

$$K_h = K_a = \frac{2\pi C}{L} \qquad \text{(C-27a)}$$

where

$$C = \frac{8(1-\nu)}{(3-4\nu)}Gd = \frac{4(1-\nu)}{(3-4\nu)(1+\nu)}Ed \quad . \qquad \text{(C-27b)}$$

The reason for this form will become apparent later in this discussion.

Design Forces Due to Transverse-Horizontal Shear Waves

The maximum values for the bending moment, shear force, pressure, and axial force are given by Equations (C-18–C-21). The expressions for design forces are found by maximizing these equations with respect to the wavelength. In the following, the expressions for design forces are derived for two cases. In one case the foundation modulus is assumed to be constant or independent of the wavelength, while in the other it is assumed to be a function of the wavelength and is given by Equation (C-27). The purpose is to study the effect of the variation of the foundation modulus on the design values, as the expression for the foundation modulus derived in the above section may not apply in some cases.

The design value for the bending moment is obtained by setting $\partial M/\partial L = 0$ in Equation (C-18). If the foundation modulus is assumed to be independent of L, the value of the wavelength that will maximize the value of the bending moment is given by

$$L_{m_1} = 2\pi\left(\frac{E'I}{K_h}\right)^{1/4} \qquad \text{(C-28)}$$

and the bending moment is given by

$$\mathrm{M}_{d_1} = \frac{1}{2}(K_h E' I)^{1/2}\,A \quad . \qquad \text{(C-29)}$$

On the other hand, if K_h is assumed to be a function of the wavelength, L, as given by Equation (C-27), then the value of the wavelength that will satisfy the condition $\partial M/\partial L = 0$ is given by

$$L_{m_2} = 2\pi\left(\frac{E'I}{2C}\right)^{1/3} \qquad \text{(C-30)}$$

and the bending moment is given by

$$\mathrm{M}_{d_2} = \frac{1}{3}(4\,E'IC^2)^{1/3}\,A \qquad \text{(C-31)}$$

where C is given by Equation (C-27b). These equations for the wavelength and bending moment can be rewritten as

$$L_{m_2} = 2\pi\left(\frac{E'I}{2K_h}\right)^{1/4} \qquad \text{(C-32)}$$

and

$$\mathrm{M}_d = \frac{\sqrt{2}}{3}(E'\,I\,K_h)^{1/2}\,A \qquad \text{(C-33)}$$

in order to compare them with the corresponding equations derived for the case where K_h is assumed to be independent of the wavelength. It is interesting to note that the values of the bending moment given by Equations (C-29) and (C-33) are within 10%.

For the shear force, the value of the wavelength that satisfies the condition $\frac{\partial V}{\partial L} = 0$ when K_h is assumed to be independent of L is given by

$$L_{v_1} = 2\pi\left(\frac{E'I}{3K_h}\right)^{1/4} \qquad \text{(C-34)}$$

and the shear force is given by

$$\mathrm{V}_{d_1} = \frac{3}{4}\,(\tfrac{1}{3}E'\,I\,K_h{}^3)^{1/4}\,A \quad . \qquad \text{(C-35)}$$

In the case where K_h is assumed to be a function of the wavelength, the shear force is maximum for L equal to zero and is given by

$$V_{d_2} = CA \qquad \text{(C-36)}$$

where C is given by Equation (C-27b).

For the pressure, the value of the wavelength that satisfies the condition $\frac{\partial P}{\partial L} = 0$ when K_h is assumed to be independent of L is equal to zero, and the pressure is given by

$$P_{d_1} = K_h\,A \quad . \qquad \text{(C-37)}$$

In the case where K_h is assumed to be a function of the wavelength, the pressure is maximum for

$$L_{p_2} = 2\pi\left(\frac{E'I}{4K_h}\right)^{1/4} = 2\pi\left(\frac{E'I}{4C}\right)^{1/3} \qquad \text{(C-38)}$$

and is given by

$$P_{d_2} = \frac{4}{5}K_h\,A = \frac{4}{5}\left(\frac{4C^4}{E'I}\right)^{1/3}A \qquad \text{(C-39)}$$

where C is given by Equation (C-27b).

For the axial force, the value of the wavelength that satisfies the condition $\partial Q/\partial L = 0$ when K_a is assumed to be independent of L is given by

$$L_{Q_1} = 2\pi\left(\frac{E'A_c}{2}\right)^{1/2} \qquad \text{(C-40)}$$

and the axial force is given by

$$Q_{d_1} = \frac{1}{4}(2\,E'A_c\,K_a)^{1/2}\,A \quad . \qquad \text{(C-41)}$$

In the case where K_a is assumed to be a function of the wavelength, the axial force is maximized for L equal to zero and is given by

$$Q_{d_2} = CA \qquad \text{(C-42)}$$

where C is given by Equation (C-27b).

The design forces resulting from transverse-horizontal shear waves are summarized in Table 6 for the two cases under consideration. It is recommended that the equations derived for the second case, or the case where the foundation modulus is assumed to be a function of the wavelength, be used unless it is believed that the approach used to derive the foundation modulus does not apply for the case under consideration.

Forces Due to Vertical Shear Waves

The same procedure described above for the case of transverse-horizontal shear waves can be applied to the case of vertical shear waves. As a result, the forces acting on the tunnel structure due to a vertical shear wave are also given by Equations (C-18–C-21). However, the value of the foundation modulus and the wave amplitude should correspond to that of a vertical shear wave.

Foundation Modulus Under a Vertical Load

In the case of a transverse-horizontal shear wave, a singular solution in elasto-statics corresponding to a line load in an infinite, homogeneous, isotropic, elastic medium was used to derive an expression for the foundation modulus. In the case of a vertical load, the above assumption of an infinite medium may not apply if the soil medium above the tunnel structure is much softer than the soul medium below it. Thus, it is preferable to use a solution based on a load on a semi-infinite medium. A solution similar to that of Kelvin's problem but for a load on a semi-infinite medium exists and is known as the Flamant's problem. In this case the vertical displacement u_y due to a vertical concentrated force can be written as

$$u_y = -\frac{(1-\nu)}{2\pi G}\,\sigma_y\,[ln\,|x| - ln\,|a|] \qquad \text{(C-43)}$$

where a is a constant and corresponds to a rigid body motion. It should be noted that the above equation is similar to Equation (C-22) and as a result, the same solution procedure used in the previous problem applies. As a result, the foundation modulus is given by

$$K_v = \frac{2\pi G}{(1-\nu)}\,\frac{d}{L} \qquad \text{(C-44)}$$

which can be written in a more convenient way as

$$K_v = \frac{2\pi B}{L} \qquad \text{(C-45a)}$$

where

$$B = \frac{Gd}{(1-\nu)} = \frac{Ed}{2(1-\nu)(1+\nu)} \quad . \qquad \text{(C-45b)}$$

Table 6. Design forces resulting from transverse-horizontal shear waves.

Case 1. Foundation modulus is independent of the wavelength

Bending moment $= \frac{1}{2}(K_h E'I)^{1/2} A$

Shear force $= \frac{3}{4}(\frac{1}{3} K_h^3 E'I) A$

Pressure $K_h A$

Axial force $= \frac{1}{4}(2 K_a E'A_c)^{1/2} A$

Case 2. Foundation modulus is a function of the wavelength

Bending moment $= \frac{\sqrt{2}}{3}(K_h E'I)^{1/2} A = \frac{1}{3}(4 C^2 E'I)^{1/3} A$

Shear force $= CA$

Pressure $= \frac{4}{5} K_h A = \frac{4}{5}\left(\frac{4B^4}{E'I}\right)^{1/3} A$

Axial force $= CA$

E' = modulus of elasticity of tunnel structure
A_c = area of tunnel cross-section
I = moment of inertia of tunnel cross-section
d = width of tunnel
E = modulus of elasticity of soil medium
ν = Poisson's ratio of soil medium
K_h = foundation modulus for transverse-horizontal load
K_a = foundation modulus for axial load

$$C = \frac{4(1-\nu)}{(3-4\nu)(1+\nu)} Ed$$

Design Forces Due to Vertical Shear Waves

The same procedure used above, in "Design Forces Due to Transverse-Horizontal Shear Waves," to obtain the design values for the bending moment, shear force and pressure when the structure is subjected to transverse-horizontal shear waves applies for the case of vertical shear waves. Only the constant C, which appears in the equation for the foundation modulus, should be replaced by its equivalent B, which was derived in the above section. As a result, the design values for the case are given by

$$M_d = \frac{1}{3}(4\,E'IB^2)^{1/3} A \qquad \text{(C-46)}$$

$$V_d = B\,A \qquad \text{(C-47)}$$

$$P_d = \frac{4}{5}\left(\frac{4B^4}{E'I}\right)^{1/3} A \qquad \text{(C-48)}$$

where $B = Gd/(1-\nu)$.

The design value for the axial force is the same as that given by Equation (C-42), since the foundation modulus in the axial direction is the same as that in the case of transverse horizontal shear waves. The axial force is thus equal to

$$Q_d = CA \qquad \text{(C-49)}$$

where $C = 8(1-\nu)\,Gd/(3-4\nu)$.

In all of the above expressions, the value of the displacement amplitude A is obtained from the design spectrum for vertical shear waves or taken equal to 1/2 to 2/3 of the displacement due to transverse-horizontal shear waves.

Forces Due to Compressional Waves

The same approach used to analyse a tunnel structure subjected to a shear wave can be used to study the effects of a compressional wave. In this case, the curvature of the structure is given

$$\frac{1}{\rho} = \left(\frac{2\pi}{L}\right)^2 \sin\phi\cos\phi\,A\,\sin\left(\frac{2\pi x}{L/\cos\phi}\right)^4. \qquad \text{(C-50)}$$

It is apparent by comparing the above equation to Equation (C-3) that the curvature of the tunnel structure due to a compressional wave is smaller than that due to a shear wave. As a result, the bending moment and shear force in the tunnel are smaller when the structure is subjected to a P-wave than when it is subjected to a S-wave.

When subjected to a P-wave, the tunnel structure also will experience an axial deformation, given by

$$u_x = A\cos\phi\,\sin\left(\frac{2\pi x}{L/\cos\phi}\right) \quad . \qquad \text{(C-51)}$$

As in the case of S-waves, the theory of an elastic beam on an elastic foundation yields a reduction factor for the axial deformation given by

$$R_2 = \frac{1}{1 + \frac{E' A_c}{K_a} \left(\frac{2\pi}{L}\right)^2 \cos^2 \phi} \quad . \quad \text{(C-52)}$$

The axial force is thus equal to

$$Q = \frac{\frac{2\pi}{L} \cos \phi}{1 + \frac{E' A_c}{K_a} \left(\frac{2\pi}{L}\right)^2 \cos^2 \phi} \quad \text{(C-53)}$$

$$E' A_c . A . \sin \left(\frac{2\pi x}{L/\cos \phi}\right) \quad .$$

The maximum value for the axial force is obtained by setting (a) $\sin \left(\frac{2\pi x}{L/\cos \phi}\right)$ equal to one, and (b) $\partial Q/\partial \phi = 0$. The angle of incidence that satisfies the second condition is equal to zero, which results in a wave parallel to the axis of the structure. As a result, the maximum axial force is given by

$$Q = \frac{\frac{2\pi}{L}}{1 + \frac{E' A_c}{K_a} \left(\frac{2\pi}{L}\right)^2} E' A_c . A \quad . \quad \text{(C-54)}$$

The above expression needs to be maximized with respect to the wavelength, L. Again, two cases will be considered. The first case corresponds to a foundation modulus, K_a, equal to a constant or independent of the wavelength. The second case corresponds to a foundation modulus that is a function of the wavelength and is given by Equation (C-27). In the first case, the value of the wavelength that satisfies the condition $\partial Q/\partial L = 0$, is given by

$$L_{Q_1} = 2\pi \left(\frac{E' A_c}{K_a}\right)^{1/2} \quad \text{(C-55)}$$

and the axial force is given by

$$Q_{d_1} = \frac{1}{2} (K_a E' A_c)^{1/2} A. \quad \text{(C-56)}$$

In the case where the foundation modulus is given by Equation (C-27), the value of the wavelength that will maximize the axial force is equal to zero and the axial force is given by

$$Q_{d_2} = CA \quad \text{(C-57)}$$

where C is given by Equation (C-27b).

It is apparent that both assumptions for the foundation modulus yields the same value for the axial force. This above expression is also the same as that obtained for a tunnel structure subjected to a shear wave. However, in this case the value of the displacement amplitude, A, corresponds to that of compressional waves; this value is, in general, smaller than that for shear waves. As a result, the maximum bending moments, shear and axial forces in the tunnel structure are, in general, caused by shear waves.

Appendix D—Applications

Three examples on the seismic design of underground structures are included in order to illustrate the application of the methodology described in this report. One example is for the case where the structure is stiff compared to the surrounding medium and it resists the ground motion; the other two are for the case where the structure is flexible compared to the surrounding medium and it conforms to the ground motion.

Example of a Structure that Resists Ground Motion

To illustrate the application of the methodology developed for structures that resist ground motion, the design conditions for the Trans-Bay Tube of the San Francisco Bay Area Rapid Transit (SFBART) system are considered (Parsons Brinckerhoff 1960). The properties of the submerged tube and the surrounding soil medium are summarized in Fig. 24. The solution procedure involves three steps: (1) calculation of maximum forces due to transverse horizontal shear waves; (2) calculation of maximum forces due to vertical shear waves; and (3) calculation of design forces due to combined effects of horizontal and vertical shear waves. The operations involved in the first and second steps are illustrated in Tables 7 and 8, respectively. The maximum values of the bending moment, shear, and axial forces are then combined using the square root of the sum of the squares of the values calculated in Steps 1 and 2, to obtain the design value (Step 3) for each quantity. The design values are summarized in Table 9.

The design forces calculated using the recommended design procedure compare very well with those calculated in the actual preliminary design analysis of the Trans Bay Tube, provided that the same displacement amplitudes given by Parsons Brinckerhoff (1960) are used. No attempt has been made to redefine the seismic environment for this structure. In this example, ground/structure interaction reduced the maximum bending moment and shear force applied on the structure by a factor of 3 and 2, respectively.

Unlined Excavation in Rock

This example considers whether special ground support would be required for underground excavations in welded tuff, at a site at which the peak particle velocity due to an earthquake is estimated to be 28 cm/s. The P-wave velocity and density for the welded tuff are estimated to be 3000 m/s and

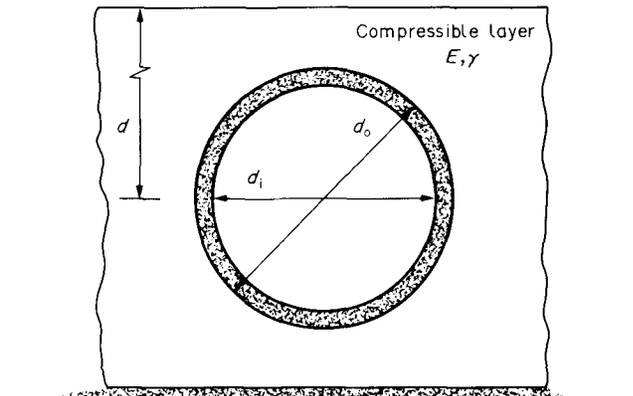

Tube properties	Soil propertieses
d_i = 29 ft 4 in.	E (psf) = 372000 + 68500 /d (ft)
d_o = 35 ft	υ = 0.49
E' = 4.32 x 10^8 lb/ft^2	d = 60 ft
$A_c = \frac{\pi}{4}(d_o^2 - d_i^2)$ = 286 ft^2	E = 3.738 x 10^6 lb/ft^2
$I = \frac{\pi}{64}(d_o^4 - d_i^4)$ = 3.73 x 10^4 ft^4	
$E'I$ = 1.611 x 10^{13} lb-ft^2	

Figure 24. Illustrative problem: SFBART trans-bay tube cross-section.

Table 7. Design forces due to transverse-horizontal shear waves illustrative calculation - SFBART.

$$C = \frac{4(1-\nu)}{(3-4\nu)(1+\nu)} Ed = \frac{4(1-0.49)}{(3-4\times0.49)(1+0.49)} 3.738 \times 10^6 \times 35$$

$C = 1.722 \times 10^8$ lb/ft

$M_d = 1/3\,(4E'IC^2)^{1/3} A = 1/3\,(4 \times 1.611 \times 10^{13} \times (1.722 \times 10^8)^2)^{1/3} A$

$M_d = 4.14 \times 10^9 A$ lb-ft

$V_d = C A = 1.722 \times 10^8 A$ lb

$Q_d = C A = 1.722 \times 10^8 A$ lb

$$P_d = 4/5 \left(\frac{4C^4}{E'I}\right)^{1/3} A = 4/5 \left(\frac{4\,(1.722 \times 10^8)^4}{1.611 \times 10^{13}}\right)^{1/3} A$$

$P_d = 4.82 \times 10^6 A$ lb/ft

If the values of the amplitude, A, obtained for the SFBART are used, then the design forces are given by:

$M_d = 4.14 \times 10^9 \times 0.01854 = 7.68 \times 10^7$ lb-ft

$V_d = 1.722 \times 10^8 \times 0.01144 = 1.97 \times 10^6$ lb

$P_d = 4.82 \times 10^6 \times 0.00786 = 3.79 \times 10^4$ lb/ft

The corresponding values for SFBART were respectively 7.78×10^7 lb-ft, 1.69×10^6 lb and 4.93×10^4 lb/ft.

Table 8. Forces due to vertical shear waves illustrative calculation - SFBART.

$$B = \frac{Ed}{2(1-\nu)(1+\nu)} = \frac{3.738 \times 10^6 \times 35}{2(1-0.49)(1+0.49)} = 8.608 \times 10^7 \text{ lb/ft}$$

$$M_d = \frac{1}{3}\,(4 \times 1.611 \times 10^{13} \times (8.608 \times 10^7)^2)^{1/3} A$$

$M_d = 2.61 \times 10^9 A$ lb-ft

$V_d = 8.61 \times 10^7 A$ lb

$Q_d = 8.61 \times 10^7 A$ lb

$$P_d = \frac{4}{5} \left(\frac{4(8.608 \times 10^7)^4}{1.611 \times 10^{13}}\right)^{1/3} A = 1.91 \times 10^6 A \text{ lb/ft}$$

If the values of the amplitude, A, are assumed to be equal to 2/3 of those for the transverse-horizontal shear wave, then the design forces are given by:

$M_d = 2.61 \times 10^9 \times 0.01236 = 3.23 \times 10^7$ lb-ft

$V_d = 8.61 \times 10^7 \times 0.00763 = 6.57 \times 10^5$ lb

$P_d = 1.91 \times 10^6 \times 0.00524 = 1.0 \times 10^4$ lb/ft

The corresponding values for SFBART were respectively 5.06×10^7 lb-ft, 1.04×10^6 lb and 2.8×10^4 lb/ft.

Table 9. Combined effect of horizontal and vertical shear waves.

$M_d = ((7.68 \times 10^7)^2 + (3.23 \times 10^7)^2)^{1/2} = 8.33 \times 10^7$ lb-ft

$V_d = ((1.97 \times 10^6)^2 + (6.57 \times 10^5)^2)^{1/2} = 2.08 \times 10^6$ lb

The corresponding values for SFBART were, respectively, 9.28×10^7 lb-ft and 1.98×10^6 lb.

2.2 g/cm^3, respectively. From Table 1, the peak longitudinal and normal strains resulting from a P-wave will be:

$$\epsilon_m = \pm \frac{V_p}{c_p} \cong \pm 1.0 \times 10^{-4} \quad .$$

The corresponding normal stress is, from Table 2

$$\sigma_m = \pm \frac{(1-\nu)E}{(1+\nu)(1-2\nu)} \frac{V_p}{cp}$$

$$= \pm \rho\, c_p^2\, \epsilon_m \cong \pm 2 \text{ MPa}$$

where the designation ± has been adopted to denote the fact that the stresses are superimposed upon the initial field stresses.

The potential significance of the induced stresses will depend very much upon the initial stresses. In the case under consideration, the excavations are relatively deep, and the pre-excavation vertical stresses are in the range of 7-9 MPa. Although the pre-excavation horizontal stresses have not been measured, it is very likely that they exceed estimated peak seismic loading of 2 MPa. In that case, P-waves propagating parallel to the tunnels would be unlikely to cause serious loosening of the roof. P-waves propagating perpendicular to the tunnel axis could temporarily result in low total horizontal stresses, with some potential for joint opening and joint shear displacement. The rock support system should be designed to be sufficient to inhibit large block movements and minor rock falls. In view of the rather low peak ground motions and total stress, rockbolts and wire mesh would probably prove to be satisfactory.

Underground Box Structure in Soil

In this example we consider the interaction between soil and an under-

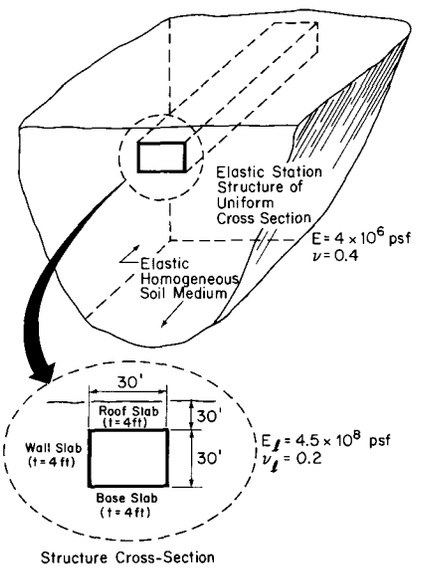

Figure 25. Basic soil/structure system.

ground box-type structure (illustrated in Fig. 25). To investigate interaction effects, two types of analyses were performed. First, the rocking deformation of the box structure was evaluated by performing analyses of a plane cross-section of the structure within the soil. Racking deformation was induced in the soil by applying graded horizontal displacements at remote, vertical boundaries of the models (Fig. 26). To avoid problems associated with attempting to induce uniform shear deformation throughout the soil medium through applying boundary displacements, analyses were performed with and without the model of the box structure.

The second model comprised a three-dimensional box structure with sinusoidally varying deformation applied to the remote soil boundaries (Fig. 27). The objective of that analysis was to investigate the extent to which the box-type structure would conform to the displacements induced by a shear wave propagating parallel to the long axis of the structure.

Both the two- and three-dimensional analyses employed finite element codes. In all cases, loading was applied statically.

When the material properties defined in Fig. 25 were used, the two-dimensional soil-structure interaction calculations predicted racking deformations in the structure that were approx. 50% of the free-field deformation, i.e. the deformations were 50% of those that would occur if there were no structure. When the soil modulus was increased by a factor of two, the formation of the structure increased to approx. 60% of the free-field values. When the flexibility of the structure was increased by reducing the wall thickness from 4 to 2 ft, the rocking deformations increased to 55 and 65% of the free-field values for the two soil stiffness.

The three-dimensional analysis of the shear wave propagating parallel to the axis of the structure provided results very similar to those described above: the deformation of the structure was approx. 50% of the free-field value for the case depicted in Fig. 25. Subsequent analyses have indicated that the reduction factor is sensitive to the wavelength.

The results of all these analyses suggest, therefore, that it may be very conservative to design a structure to accommodate all the shear deformation in the free-field. If such conservatism leads to conclusions that significant design modifications would be required because of seismic loading, then relatively simple calculations of the type described above can be used to refine and reduce the seismic design loads.

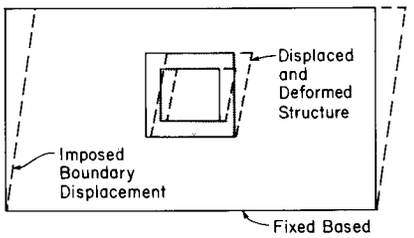

Figure 26. Schematic of deformation of box structure cross-section.

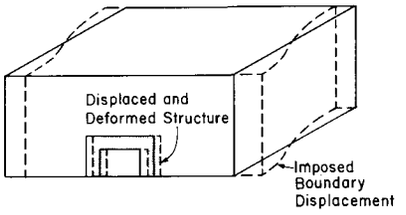

Figure 27. Schematic of deformation to simulate horizontally propagating shear wave.